Preprints.org

Article

Not peer-reviewed version

Human miRNA Expression and Plant miRNA: A Statistical Approach for Cancer Therapy

Maksym Zoziuk , Vittorio Colizzi , Maurizio Mattei , Pavlo Krysenko , Roberta Bernardini , Fabio Massimo Zanzotto , Stefano Marini , Dmitri Koroliouk *

Posted Date: 6 June 2025

doi: 10.20944/preprints202506.0520.v1

Keywords: miRNA; cancer; expression analysis; target genes; plant miRNAs; bioinformatics; statistical distribution

Preprints.org is a free multidisciplinary platform providing preprint service that is dedicated to making early versions of research outputs permanently available and citable. Preprints posted at Preprints.org appear in Web of Science, Crossref, Google Scholar, Scilit, Europe PMC.

Copyright: This open access article is published under a Creative Commons CC BY 4.0 license, which permit the free download, distribution, and reuse, provided that the author and preprint are cited in any reuse.

Preprints.org (www.preprints.org) | NOT PEER-REVIEWED | Posted: 6 June 2025 doi:10.20944/preprints202506.0520.v1

Disclaimer/Publisher's Note: The statements, opinions, and data contained in all publications are solely those of the individual author(s) and contributor(s) and not of MDPI and/or the editor(s). MDPI and/or the editor(s) disclaim responsibility for any injury to people or property resulting from any ideas, methods, instructions, or products referred to in the content.

Article

Human miRNA Expression and Plant miRNA: A Statistical Approach for Cancer Therapy

Maksym Zoziuk [1], Vittorio Colizzi [2], Maurizio Mattei [1,3], Pavlo Krysenko [4], Roberta Bernardini [5], Fabio Massimo Zanzotto [6], Stefano Marini [5] and Dmitri Koroliouk [1,4,7,8,*]

[1] Centro Interdipartimentale di Medicina Comparata, Tecniche Alternative ed Acquacoltura, Interdepartmental Center for Comparative Medicine, Alternative Techniques, and Aquaculture, University of Rome Tor Vergata, Via Montpellier 1, 00133 Rome, Italy
[2] UNESCO Chair in Interdisciplinary Biotechnology, University of Rome Tor Vergata, Via della Ricerca Scientifica 1, 00173 Rome, Italy
[3] Department of Biology, University of Rome Tor Vergata, Via della Ricerca Scientifica 1, 00173 Rome, Italy
[4] Institute of Telecommunications and Global Information Space of the National Academy of Sciences of Ukraine, Chokolivskiy bulv. 13, 03186 Kyiv, Ukraine
[5] Faculty of Medicine, Department of Clinical Sciences and Translational Medicine, University of Rome Tor Vergata, Via Montpellier 1, 00133 Roma, Italy
[6] Department of Business Engineering "Mario Lucertini", University of Rome Tor Vergata, Via del Politecnico, 1, 00133 Rome, Italy
[7] Department of Microelectronics, Faculty of Electronics, National Technical University of Ukraine "Igor Sikorsky Kyiv Polytechnic Institute", Beresteiska Ave. 37, 03056 Kyiv, Ukraine
[8] Institute of Mathematics of the National Academy of Sciences of Ukraine, 3, Tereschenkivska St., 01004 Kyiv, Ukraine
* Correspondence: dimitri.koroliouk@ukr.net or krldtr01@uniroma2.it

Abstract: Background/Objectives: The regulatory role of miRNAs in cancer is well recognized, but most studies are confined to specific cancer types or individual miRNAs. This study aims to identify miRNAs involved in global oncological mechanisms that transcend individual cancer types. **Methods:** We analyzed expression data from all known human miRNAs across all cancer types. A statistical approach was developed and expression distributions to define miRNAs with under- or over-expression patterns. We then studied miRNA-target gene relationships and investigated complementarity between human and plant miRNAs to propose potential therapeutic plant miRNA panels. **Results:** Critical miRNAs were identified based on their expression trends and impact on target genes. Plant miRNAs with strong complementarity to underexpressed human miRNAs and weak complementarity to overexpressed miRNAs were selected as candidates for therapeutic panels. Distribution patterns and key correlations were visualized using figures. **Conclusions:** The results suggest that a approach for making panels of selected plant miRNAs may offer therapeutic benefit by compensating for deficiencies in human miRNA expression associated with cancer. This work provides a framework for future experimental validation and therapy design.

Keywords: miRNA; cancer; expression analysis; target genes; plant miRNAs; bioinformatics; statistical distribution

1. Introduction

MicroRNAs (miRNAs) are small non-coding RNAs that modulate gene expression post-transcriptionally, primarily through interaction with messenger RNAs (mRNAs), thereby indirectly influencing DNA replication and protein synthesis[1]. They are evolutionarily conserved across plants and animals, exhibit high stability, and can be transported to specific sites to exert regulatory

© 2025 by the author(s). Distributed under a Creative Commons CC BY license.

Preprints.org (www.preprints.org) | NOT PEER-REVIEWED | Posted: 6 June 2025 doi:10.20944/preprints202506.0520.v1

effects. Recent studies have suggested that exogenous plant miRNAs may compensate for dysregulated human miRNAs, provided sufficient sequence complementarity — typically a minimum of 50% — to ensure mRNA targeting capacity[2]. To substitute one plant miRNA for another, however, a higher similarity threshold of 80–90% is usually required[3–5]. This property, termed biological complementarity, underpins the potential interchangeability of miRNAs across species.

Alterations in miRNA concentrations are a hallmark of numerous cancers, yet most investigations have focused on individual miRNAs or small, disease-specific subsets[6–8]. Expression levels are typically measured in tissue and circulating blood, comparing diseased and healthy samples. Cancers frequently induce widespread perturbations in miRNA expression, leading to the hypothesis that restoring miRNA homeostasis may influence disease progression[9,10].

To explore global trends in miRNA dysregulation associated with cancer, we analyzed a comprehensive dataset containing miRNA expression profiles across multiple cancer types[11,12]. Employing machine learning, we attempted to predict miRNA expression status (under- or overexpressed) using neural networks. Despite leveraging large-scale data, classification accuracy plateaued at 70–75%, suggesting either insufficient mechanistic understanding or the influence of multiple latent variables. These results highlight the limitations of current predictive models for miRNA expression.

To bypass these constraints, we characterized each miRNA statistically, representing it by two parameters: the number of expression measurements (experiments) and a derived membership ratio (div). This enabled visualization of miRNA distributions across cancers. miRNAs with high absolute div values and extensive experimental coverage were considered strong candidates for functional relevance. These findings offer a basis for prioritizing miRNAs in targeted analyses.

We then assessed the feasibility of correcting aberrant human miRNA expression using plant miRNAs, based on average sequence complementarity. miRNAs with high div values (indicative of consistent dysregulation) were stratified by whether they were over- or underexpressed. For each plant miRNA, we computed average complementarity with both groups and identified candidates with maximal differential affinity — favoring underexpressed targets while avoiding overexpressed ones. These metrics form the foundation for evaluating therapeutic potential.

Given the vast number of dysregulated miRNAs, we further prioritized targets by identifying key genes under miRNA control. We limited our analysis to experimentally validated miRNA–gene interactions. Since one gene may be regulated by multiple miRNAs, we computed, for each gene, the number of regulating miRNAs and the aggregated div metric of these miRNAs. This allowed us to identify genes under robust miRNA-mediated regulation. Parallel expression datasets from cancer samples[17] provided direct gene-level expression data. By comparing miRNA-derived and empirical gene expression patterns, we examined consistency in regulatory trends. While many genes showed discordant profiles, others exhibited concordant regulation, suggesting differential miRNA involvement in gene expression control.

Focusing on the top 200 genes most strongly affected by both direct expression changes and miRNA-derived div metrics, we mapped back to the regulating miRNAs. From this refined miRNA set, we again computed average complementarity with plant miRNAs. Those plant miRNAs showing the largest positive differential (strong affinity for underexpressed miRNAs and weak for overexpressed) emerged as optimal candidates for therapeutic intervention. Conversely, plant miRNAs with the largest negative differential may inform mechanisms of cancer-promoting miRNA overabundance.

We also evaluated average complementarity at the plant-species level but observed minimal variation (<0.05%), suggesting that species-level generalizations are currently infeasible. This may reflect the sensitivity of plant miRNA profiles to cultivar, geography, and growth conditions.

Nevertheless, our framework provides a rational basis for the design of synthetic miRNAs with enhanced specificity — engineered to maximize complementarity with target human miRNAs while minimizing off-target interactions — opening avenues for future miRNA-based therapeutics.

© 2025 by the author(s). Distributed under a Creative Commons CC BY license.

Preprints.org (www.preprints.org) | NOT PEER-REVIEWED | Posted: 6 June 2025 doi:10.20944/preprints202506.0520.v1

2. Materials and Methods

Statistical analyses of miRNA expression data were performed utilizing a comprehensive database comprising multiple parameters, including cancer type, experimental modality, T-value/B-value metrics, and log fold change (logFC) [12]. The principal variable of interest was logFC, representing the logarithmic deviation of miRNA expression levels relative to baseline in tissue or blood samples. Each miRNA was profiled across numerous experiments, yielding a dataset encompassing 3,174 distinct miRNAs and 155,417 total experimental observations.

Initial analytical steps involved deploying a neural network model to predict both the quantitative logFC values and the qualitative directionality of expression changes (upregulation or downregulation). Predictions were generated for diverse sample representations, including individual miRNA measurements and mean expression profiles. Model performance was evaluated through training on input features comprising miRNA sequence data (mature and precursor forms), disease classification, experimental context, and ancillary variables.

Data processing, sorting, and visualization were conducted using custom software implemented in Python 3 within the PyCharm IDE (version 2022.1). The membership ratio was computed following the formula described in [106].

$$div = (\text{num\_of\_down} - \text{num\_of\_up})/(\text{num\_of\_down} + \text{num\_of\_up}) \quad (1)$$

where num_of_down and num_of_up denote the number of experiments in which the miRNA was significantly down- or upregulated, respectively.

It is established that each miRNA regulates a large number of target genes, and elucidating the specific mechanisms of these interactions is a crucial task, particularly regarding the interdependencies of factors, i.e., correlations of quantitative features. Databases of miRNAs and their target genes, such as miRDB [103] and miRTarBase [104], provide useful resources for this purpose. The former database includes both experimentally validated target genes and predicted miRNA-gene relationships, thereby expanding the dataset. The latter contains only experimentally validated miRNA-gene interactions. We utilized miRTarBase to identify genes associated with varying numbers of critically up- and downregulated miRNAs, as determined by the third (III) nonlinear critical threshold (Figure 2). Gene expression data for multiple cancer types were obtained from the database in [17]. Additionally, the plant miRNA database [105], comprising 10,898 plant miRNAs, was employed.

3. Results

3.1. Identification of Critical miRNAs

Neural network training results indicate that prediction accuracy for the direction of expression achieves a minimum of approximately 50% and does not exceed ~65% when considering all miRNAs. Numerical experiments applying various filters—such as restricting analysis to specific tumor types or experimental modalities—yielded similar accuracy. When focusing solely on individual miRNAs characterized by a predominance of either underexpression or overexpression (based on percentage ratio) and supported by a sufficient number of experiments to establish a trend, accuracy improves to 70–80% [16].

From these findings, several assumptions can be made:

1. Input variables—such as miRNA sequences, disease type, and experiment type—play a role but do not fully capture the overall miRNA expression profile, indicating that not all relevant information influencing expression prediction is accounted for.
2. The number of distinct miRNAs studied may be insufficient.
3. The expression data in the database may contain measurement errors.

Thus, a statistical approach is warranted to identify existing dependencies within the expression data and uncover opportunities to extract useful information about miRNAs, particularly regarding

© 2025 by the author(s). Distributed under a Creative Commons CC BY license.

Preprints.org (www.preprints.org) | NOT PEER-REVIEWED | Posted: 6 June 2025 doi:10.20944/preprints202506.0520.v1

specific miRNA sequences. Given the multitude of parameters influencing miRNA expression, it is necessary to analyze expression data collectively rather than on an experiment-by-experiment basis.

Accordingly, each miRNA was evaluated in the context of all experiments in which it was observed. An "average" expression value for each miRNA was estimated by summing all logFC values across all experiments. The resulting data were organized into a new table containing the following columns: miRNA identifier, cumulative sum of logFC, number of experiments with negative logFC, and number of experiments with positive logFC. This procedure was applied under various filtering conditions, such as specific cancer types or experimental designs. Although the values vary slightly depending on the applied filters, the overall trend remains consistent.

The number of miRNAs predominantly exhibiting overexpression and underexpression was found to be nearly equal (1606 versus 1568). It is important to note that many miRNAs are represented by a small number of experiments. Some miRNAs demonstrate membership values around or above 95%, although the number of associated experiments does not exceed several dozen.

To summarize the classification of miRNAs based on cumulative logFC expressions across all cancer types, the data are presented in the form of a truncated table (Table 1).

Table 1. Cumulative miRNA expression values ordered by magnitude. The left section of the table lists the twenty miRNAs with the lowest cumulative expression values (underexpressed), while the right section shows the twenty miRNAs with the highest cumulative expression values (overexpressed). The first column indicates the miRNA identifier; the second column presents the sum of logFC values across all experiments; the third and fourth columns denote the number of experiments in which the miRNA was underexpressed and overexpressed, respectively. These results demonstrate a clear association between cancer presence and widespread miRNA dysregulation, reflected in distinct patterns of over- and underexpression.

miRNA	sum_log_FC	Down	up	miRNA	sum_log_FC	down	up
hsa-miR-139-5p	-256,8886988	165	34	hsa-miR-429	148,5189271	40	110
hsa-miR-139-3p	-253,6689636	145	23	hsa-miR-93-5p	161,3206615	59	185
hsa-miR-125b-1-3p	-239,8640174	104	33	hsa-miR-106b-5p	162,2069637	54	191
hsa-miR-133b	-224,7014228	142	27	hsa-miR-135b-5p	164,7171991	40	117
hsa-miR-378a-3p	-218,0534439	184	49	hsa-miR-142-3p	167,0549993	45	124
hsa-miR-125a-3p	-200,0807663	105	37	hsa-miR-191-5p	167,9664181	53	116
hsa-miR-486-5p	-183,1454502	131	32	hsa-miR-5100	168,399075	15	65
hsa-miR-873-3p	-182,7628861	72	7	hsa-miR-7-5p	168,4722294	44	122
hsa-miR-145-5p	-181,2865379	171	58	hsa-miR-103a-3p	171,422429	40	161
hsa-miR-30b-3p	-173,559201	106	31	hsa-miR-17-5p	181,9678752	59	183
hsa-miR-508-5p	-170,7541897	85	30	hsa-miR-99a-5p	187,435229	888	912
hsa-miR-4648	-168,3359797	56	10	hsa-miR-1290	188,4010193	21	90
hsa-miR-575	-165,7760472	96	35	hsa-miR-301a-3p	197,3741224	43	157
hsa-miR-6501-5p	-164,5701385	69	16	hsa-miR-130b-3p	205,3449082	46	182
hsa-miR-134-3p	-163,1082517	76	19	hsa-miR-17-3p	221,2149965	51	146
hsa-miR-1-3p	-163,0672057	118	45	hsa-miR-21-5p	232,0956337	48	185
hsa-miR-497-5p	-161,7553736	141	45	hsa-miR-18a-5p	246,50339	41	188
hsa-miR-6127	-158,2358922	51	2	hsa-miR-210-3p	258,2379838	37	167
hsa-miR-6751-5p	-157,8749887	61	7	hsa-miR-96-5p	268,8365613	27	153
hsa-miR-887-5p	-157,4227012	83	10	hsa-miR-183-5p	269,522949	31	153
hsa-miR-125b-5p	-155,0589238	143	47	hsa-miR-182-5p	269,6076375	40	155

It was observed that across all expression data, a pronounced tendency exists for the majority of miRNAs (over 70% of the total distinct miRNAs) to be classified as either predominantly overexpressed or underexpressed, independent of disease type or experimental conditions (e.g., blood-derived or cell-derived samples). This trend remains consistent even when the dataset is restricted by applying various filters.

© 2025 by the author(s). Distributed under a Creative Commons CC BY license.

Preprints.org (www.preprints.org) | NOT PEER-REVIEWED | Posted: 6 June 2025 doi:10.20944/preprints202506.0520.v1

We further compared the membership ratios derived from high-throughput expression data with those obtained from low-throughput methods [12], revealing an approximate concordance of 90% (±5%), contingent on the applied filters such as total expression counts and membership thresholds.

In the following table, we present a comparative analysis of miRNAs identified in Table 1 alongside those reported in the literature, listing miRNAs classified as overexpressed or underexpressed and comparing their corresponding statistical metrics.

Table 2. The first column lists miRNA identifiers. The second column reports the cumulative sum of expression values across all experiments. The third and fourth columns indicate the number of experiments in which the miRNA is underexpressed and overexpressed, respectively. The fifth column denotes the overall direction of expression. The sixth column provides selected literature sources reporting on the expression of each miRNA. The seventh column summarizes the established oncogenic or tumor suppressor role of the miRNA. This table demonstrates that many miRNAs have been investigated multiple times, with expression data from our analysis largely consistent with published studies. Additionally, the presence of oncogenic or tumor-suppressive effects for each miRNA is indicated where available.

miRNA	sum_logFC	num_of_down	num_of_up	expression_rate	references	known_oncomir/ tumor_suppressor
hsa-miR-17-5p	181.967875163	59	183	UP	[18–21] overexpressed	oncomir
hsa-miR-17-3p	221.214996471	51	146	UP	[18–20] overexpressed	oncomir
hsa-miR-21-3p	122.420967796	39	95	UP	[18,22–30] overexpressed	oncomir
hsa-miR-21-5p	232.095633685	48	185	UP	[18,22–33] overexpressed	oncomir
hsa-miR-25-3p	105.474276835	38	143	UP	[18,34] overexpressed	oncomir
hsa-miR-92a-2-5p	-96.775839638	57	19	DOWN	[18] overexpressed	oncomir
hsa-miR-1-3p	-163.06720567600	118	45	DOWN	[35] underexpressed	unknown
hsa-miR-146b-5p	83.35547042	58	100	UP (EVEN)	[25,36–39] overexpressed	unknown
hsa-miR-210-5p	138.099992203	46	126	UP	[40–51] overexpressed	oncomir
hsa-miR-155-3p	26.049729861	30	48	UP (EVEN)	[40–43,45–51] overexpressed	oncomir
hsa-miR-20a-3p	30.7308478730000	32	51	UP (EVEN)	[19,20] overexpressed	oncomir
hsa-miR-20a-5p	128.094901003	58	150	UP (EVEN)	[19,20] overexpressed	oncomir
hsa-miR-20b-3p	18.138542252	25	48	UP (EVEN)	[19,20] overexpressed	unknown
hsa-miR-20b-5p	89.189273862	73	131	UP (EVEN)	[19,20,52] overexpressed	unknown
hsa-miR-92b-5p	33.468787427	35	86	UP	[19,20,53] overexpressed	oncomir
hsa-miR-92b-3p	55.903127821	42	97	UP (EVEN)	[19,20,53] overexpressed	oncomir
hsa-miR-106a-5p	109.437529666	46	125	UP	[19,20] overexpressed	unknown
hsa-miR-106a-3p	55.146269153	17	43	UP	[19,20] overexpressed	unknown
hsa-miR-106b-5p	162.206963737	54	191	UP	[19,20] overexpressed	oncomir
hsa-miR-106b-3p	28.655181245999	29	57	UP (EVEN)	[19,20] overexpressed	oncomir
hsa-miR-574-3p	-89.761840835	102	42	DOWN (EVEN)	[54,55] underexpressed	unknown
hsa-miR-100-5p	-42.845381169	141	96	DOWN (EVEN)	[56–58] underexpressed	oncomir
hsa-miR-100-3p	18.257709839	33	46	EVEN	[56,57] underexpressed	oncomir
hsa-miR-125b-5p	-155.058923805	143	47	DOWN	[56,57,59] underexpressed	unknown
hsa-miR-10a-5p	18.033378321	65	62	EVEN	[60]	oncomir
hsa-miR-10a-3p	33.94121654	35	41	EVEN	[60] overexpressed	unknown
hsa-miR-302c-3p	35.479451341	15	42	UP	[61,62] overexpressed	unknown
hsa-miR-302c-5p	2.7913214050000	35	32	EVEN	[61,62] overexpressed	unknown
hsa-miR-520c-3p	14.080070734	24	29	EVEN	[61,62] overexpressed	unknown
hsa-miR-181b-3p	18.138919527	9	29	UP	[37,38] overexpressed	unknown
hsa-miR-181b-5p	56.004847604	49	99	UP (EVEN)	[37,38] overexpressed	unknown
hsa-miR-874-5p	-53.671752358	61	15	DOWN	[63] underexpressed	unknown
hsa-miR-874-3p	-43.857572139	78	37	DOWN	[63] underexpressed	unknown
hsa-miR-206	-43.896241638999	66	33	DOWN	[64] underexpressed	unknown
hsa-miR-192-5p	-14.939738841999	83	73	EVEN	[65] underexpressed	unknown
hsa-miR-34a-5p	78.603195367	54	101	UP	[37,38,66–68]	tumor suppressor
hsa-miR-34a-3p	32.856116658	42	57	EVEN	[37,38,68]	tumor suppressor
hsa-miR-16-5p	122.040722105	46	130	UP	[37,38,69] overexpressed	oncomir
hsa-miR-222-3p	79.537077385	82	119	UP (EVEN)	[58,70] underexpressed	oncomir
hsa-let-7b-3p	-131.509341304	99	34	DOWN	[71] underexpressed	unknown
hsa-let-7b-5p	-28.172177114	94	64	DOWN (EVEN)	[71] underexpressed	unknown
hsa-miR-145-5p	-181.286537884	171	58	DOWN	[72–74] overexpressed	tumor suppressor
hsa-miR-145-3p	-124.148339208	92	35	DOWN	[72–74] overexpressed	tumor suppressor
hsa-miR-27a-3p	73.096939678	57	116	UP	[69,75–77] overexpressed	oncomir

© 2025 by the author(s). Distributed under a Creative Commons CC BY license.

Preprints.org (www.preprints.org) | NOT PEER-REVIEWED | Posted: 6 June 2025 doi:10.20944/preprints202506.0520.v1

hsa-miR-96-5p	268.836561293	27	153	UP	[78,79] overexpressed	oncomir
hsa-miR-483-3p	-67.676136178	80	44	DOWN (EVEN)	[80] overexpressed	
hsa-miR-19b-3p	122.182943146	49	134	UP	[37,38,81] overexpressed	oncomir
hsa-miR-125b-5p	-155.058923805	143	47	DOWN	[56,57,59,82], underexpressed	tumor suppressor
hsa-miR-4649-5p	30.756795974	13	48	UP	[83] overexpressed	unknown
hsa-miR-2467-3p	109.959427118	5	57	UP	[83] overexpressed	unknown
hsa-miR-543	-23.65012842	57	45	EVEN	[83] overexpressed	unknown
hsa-miR-301a-3p	197.37412236	43	157	UP	[83] overexpressed	unknown
hsa-miR-3132	-6.754301139	19	15	EVEN	[83] overexpressed	unknown
hsa-miR-19a-5p	82.647646616	12	64	UP	[37,38,83] overexpressed	unknown
hsa-miR-495-3p	-27.55630123000	66	42	EVEN	[83] overexpressed	unknown
hsa-miR-21-5p	232.095633685	48	185	UP	[27,29,30,84–87] overexpressed	oncomir
hsa-miR-30a-5p	-105.284666614	137	64	DOWN	[32,33] underexpressed	unknown
hsa-miR-10b-5p	15.380943873	107	94	EVEN	[85,88] overexpressed	oncomir
hsa-miR-221-3p	104.840632196	82	115	UP (EVEN)	[85,89] overexpressed	oncomir
hsa-miR-223-5p	5.1038718289999	28	29	EVEN	[85] overexpressed	oncomir
hsa-miR-223-3p	12.148270143000	78	84	EVEN	[85] overexpressed	oncomir
hsa-miR-410-3p	-9.0977574719999	56	52	EVEN	[90–92] overexpressed	oncomir
hsa-miR-182-5p	269.607637527	40	155	UP	[79,90,91] overexpressed	oncomir
hsa-miR-182-3p	72.725021519	20	84	UP	[90,91] overexpressed	oncomir
hsa-miR-29b-3p	139.840241189	61	116	UP	[50,51] overexpressed	oncomir
hsa-miR-372-5p	16.601484109	0	17	UP	[50,51] overexpressed	oncomir
hsa-miR-372-3p	7.4439734880000	33	43	EVEN	[50,51] overexpressed	oncomir
hsa-miR-9-3p	34.288294366	56	64	EVEN	[93] overexpressed	oncomir
hsa-miR-9-5p	96.301540349	52	81	UP	[93] overexpressed	oncomir
hsa-miR-146a-3p	48.769518397	21	45	UP	[94,95] overexpressed	oncomir
hsa-miR-146a-5p	58.148256963	68	101	UP (EVEN)	[94] overexpressed	oncomir
hsa-miR-23a-3p	89.970128176	59	103	UP	[69,96–98] overexpressed	oncomir
hsa-miR-23a-5p	-73.666153025	78	24	DOWN	[69,98] overexpressed	oncomir
hsa-miR-24-3p	65.578059129	54	108	UP	[69] overexpressed	oncomir
hsa-miR-519a-3p	57.869362816	25	65	UP	[99] overexpressed	oncomir
hsa-miR-425-5p	120.239658602	34	125	UP	[69,100] overexpressed	oncomir
hsa-miR-208b-5p	23.336730899	1	26	UP	[101] overexpressed	oncomir
hsa-miR-208b-3p	10.431775042	15	27	UP	[101] overexpressed	oncomir
hsa-miR-18a-5p	246.503390015	41	188	UP	[102] overexpressed	oncomir

The following Figure 1 illustrates the distribution of all 3,173 miRNAs according to the number of experiments in which they were observed and their respective membership ratios. All miRNAs listed in Table 2 are highlighted within this overall distribution.

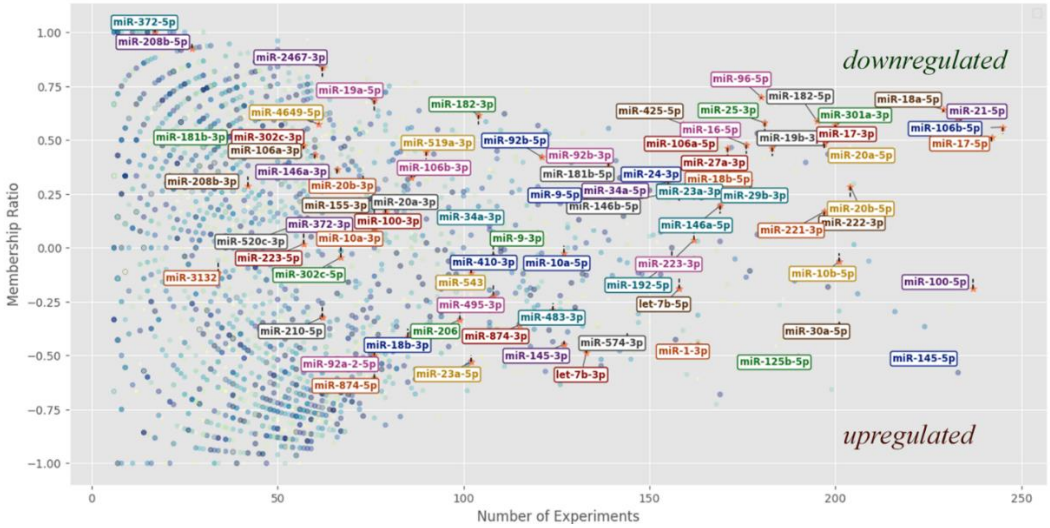

Figure 1. Distribution of individual miRNAs according to the number of experiments (X-axis) and membership ratio ("div") (Y-axis). Data points representing miRNAs observed in five or fewer experiments are excluded, reducing the dataset from 3,171 to 2,607 miRNAs. The plot demonstrates that a substantial proportion of miRNAs listed in Table 2 exhibit a clear tendency toward either overexpression or underexpression. [106].

© 2025 by the author(s). Distributed under a Creative Commons CC BY license.

Preprints.org (www.preprints.org) | NOT PEER-REVIEWED | Posted: 6 June 2025 doi:10.20944/preprints202506.0520.v1

As observed, many studied indicators exhibit a clear trend toward either upregulation or downregulation. However, numerous miRNAs remain poorly characterized with respect to the molecular mechanisms in which they participate. Additionally, as the number of experiments per miRNA increases, its position on the distribution converges toward an average value.

A key challenge lies in defining the boundary between "critical" and "non-critical" miRNAs. Multiple factors influence miRNA expression, a conclusion supported by neural network analyses. This underscores the necessity for additional contextual information regarding the experimental conditions under which miRNA expression is measured, including potentially relevant molecular mechanisms and regulatory factors.

It is evident that increasing the number of experiments enhances the robustness of correlations between miRNA expression patterns in diseased versus healthy tissues. Furthermore, a higher ratio between the number of experiments showing negative versus positive miRNA expression strengthens the statistical significance of associations between miRNA dysregulation and cancer. Balancing these parameters is complicated by substantial variability in experiment counts across individual miRNAs.

Figure 2 presents the relationship between the cumulative difference metric (div) and the number of experiments, delineating three boundary regions corresponding to nonlinear thresholds. These critical div values serve to classify general miRNA expression trends across cancer types. A color-coded scheme visually represents miRNA concentration (dots) within distinct graph regions.

Panel (b) of Figure 2 illustrates the upper threshold (I) alongside miRNAs from the table whose expression behaviors have been characterized in greater detail.

It should be noted that only a small subset of miRNAs has been studied in detail (see references in Table 2), indicating that a considerable number of human miRNAs remain insufficiently characterized with respect to their biological functions. Notably, within the nonlinear threshold I, Table 2 lists 17 out of 165 overexpressed miRNAs and only 6 out of 414 underexpressed miRNAs. This suggests that miRNAs with higher abundance have been more extensively investigated compared to those present at lower levels.

Figure 3 presents expression distributions as a function of the number of experiments for the 20 most frequently studied miRNAs within the nonlinear zone I, comprising both underexpressed and overexpressed groups.

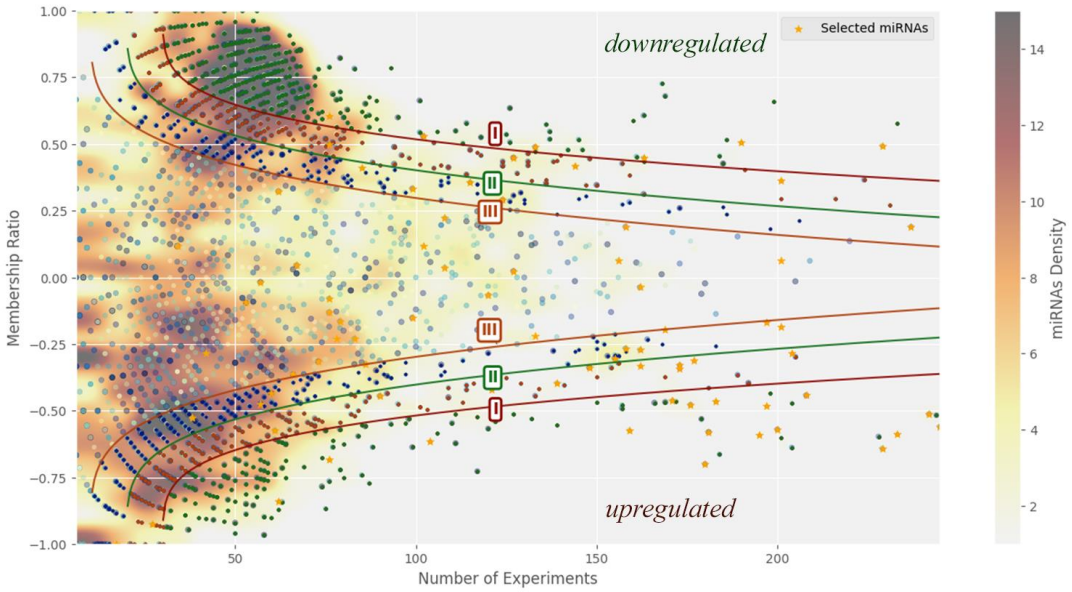

(**a**)

© 2025 by the author(s). Distributed under a Creative Commons CC BY license.

Preprints.org (www.preprints.org) | NOT PEER-REVIEWED | Posted: 6 June 2025 doi:10.20944/preprints202506.0520.v1

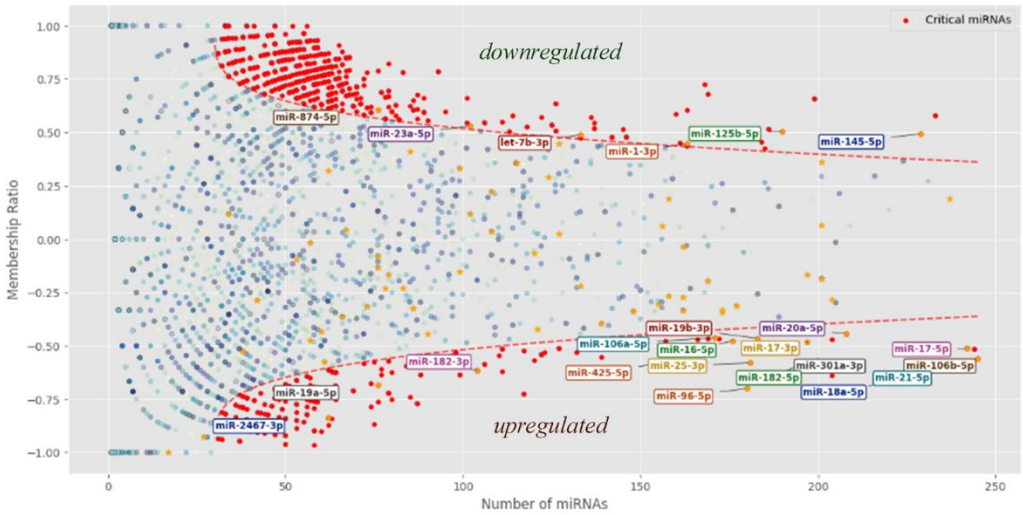

(**b**)

Figure 2. Non-linear classification of critical miRNAs. (a) Distribution plot depicting three non-linear threshold curves alongside the concentration spectrum of individual miRNAs. (b) Distribution graph showing the upper threshold curve (I) together with miRNAs reported in the literature. All threshold lines were defined based on our analytical criteria. The primary threshold line (I) identifies critical miRNAs that are of particular interest for investigating their association with cancer presence.

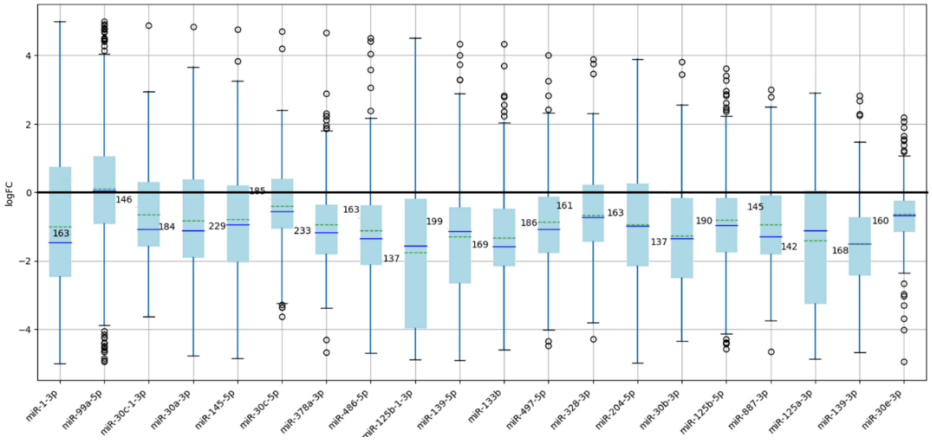

(**a**)

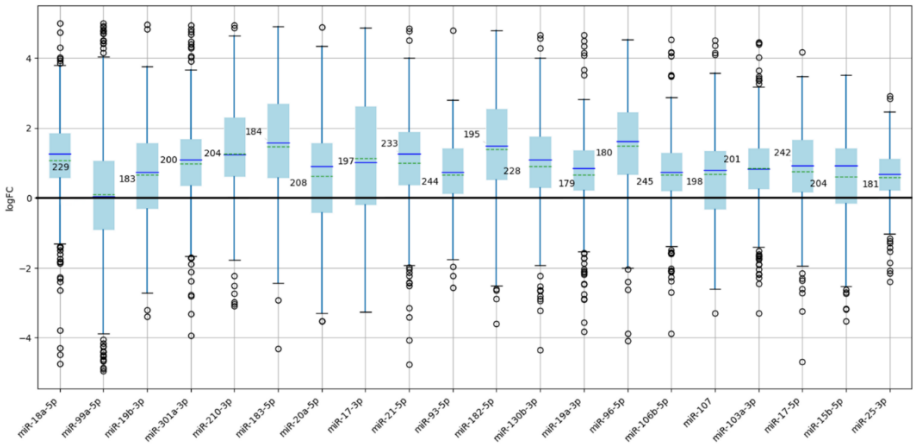

(**b**)

Figure 3. Box plots representing the distribution of expression values for the 20 underexpressed (a) and 20 overexpressed (b) miRNAs with the highest number of experiments. This selection highlights the most relevant miRNAs exhibiting average expression values significantly greater or less than zero, demonstrating a pronounced tendency toward consistent dysregulation.

© 2025 by the author(s). Distributed under a Creative Commons CC BY license.

Preprints.org (www.preprints.org) | NOT PEER-REVIEWED | Posted: 6 June 2025 doi:10.20944/preprints202506.0520.v1

It is evident that as the number of experiments assessing miRNA expression increases, the average expression value tends to converge toward a membership ratio of 0. However, there are miRNAs with between 20 and 50 experiments that maintain a membership ratio exceeding 0.7, as illustrated in Figure 4.

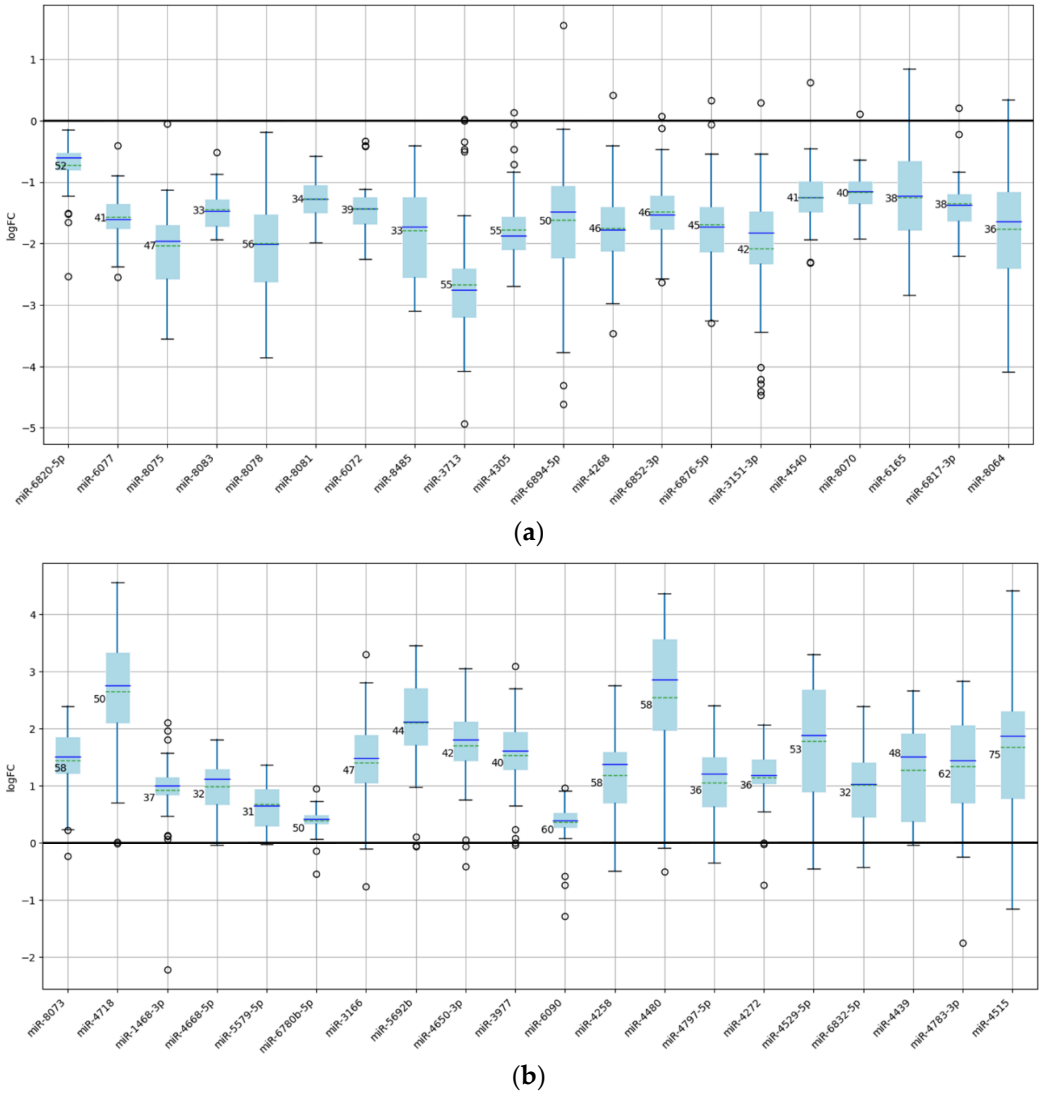

Figure 4. Box plots of miRNAs exhibiting the highest membership ratios. (a) Twenty underexpressed miRNAs. (b) Twenty overexpressed miRNAs.

Table 3 presents selected statistical parameters for overexpressed and underexpressed miRNAs. For all miRNAs exceeding the nonlinear thresholds, the table reports the number of unique miRNAs (data points), the total number of experiments aggregated across these miRNAs, and the cumulative expression values. Across all metrics, underexpressed miRNAs predominate over overexpressed ones. This disparity is especially pronounced at the primary (I) nonlinear threshold, where miRNAs above the threshold are considered more biologically relevant. Here, the dominance of underexpressed miRNAs is markedly clear.

Overall, these findings suggest that in cancerous conditions, the repertoire of underexpressed miRNAs substantially exceeds that of overexpressed miRNAs. This implies that many miRNAs exhibit markedly reduced concentrations in the presence of cancer compared to those whose levels are elevated. The underlying causes may vary: cancer could impair miRNA biogenesis pathways, reflect a host protective response to tumorigenesis, or result from a complex interplay of these and other factors.

© 2025 by the author(s). Distributed under a Creative Commons CC BY license.

Preprints.org (www.preprints.org) | NOT PEER-REVIEWED | Posted: 6 June 2025 doi:10.20944/preprints202506.0520.v1

Table 3. Summary of statistical parameters for underexpressed and overexpressed miRNAs categorized according to three nonlinear thresholds (III, II, I). This table provides a concise comparison highlighting the differences between under- and overexpressed miRNAs across these classification levels. Notably, the most pronounced disparity is observed at the primary (I) threshold.

Parameter	Nonlinear limit	DOWN critical	UP critical
Number of singular miRNAs	III	786	607
	II	615	378
	I	414	165
Number of experiments	III	51 370	38 573
	II	39 853	26 254
	I	26 235	13 896
Total sum of logFC	III	-51 466	29 037
	II	-45 134	23 071
	I	-34 315	14 493

3.2. Statistical Relationship Between miRNA and Target Genes

Statistical associations between miRNAs and their target genes were analyzed by calculating, for each gene, the number of underexpressed and overexpressed miRNAs (according to threshold III), as well as the difference between these counts (see Table 4).

Table 4. Summary of gene-targeted miRNA expression statistics. The first column lists gene names; the second column shows the total number of underexpressed miRNAs targeting each gene; the third column indicates the total number of overexpressed miRNAs; the fourth column provides the difference between these two sums for convenience; the fifth column represents the total number of miRNAs targeting the gene; and the sixth column gives the membership ratio (div parameter). The data illustrate how a substantial number of genes exhibit down- or up-regulation driven by the corresponding down- or up-regulation of their targeting miRNAs.

gene	num_of_app_DOWN	num_of_app_UP	diff	summ	div
VAV3	593	258	335	851	0,393655
AGO2	551	262	289	813	0,355474
GATA6	439	207	232	646	0,359133
MED28	265	80	185	345	0,536232
TPM3	238	62	176	300	0,586667
HHIP	267	97	170	364	0,467033
ATG2A	194	34	160	228	0,701754
PGPEP1	213	59	154	272	0,566176
SLC25A45	166	22	144	188	0,765957
gene	**num_of_app_DOWN**	**num_of_app_UP**	**diff**	**summ**	**div**
BTBD3	54	254	-200	308	-0,64935
FOXN2	48	258	-210	306	-0,68627
AKAP11	57	271	-214	328	-0,65244
MYLIP	73	289	-216	362	-0,59669
CCND1	227	447	-220	674	-0,32641
RAN	45	267	-222	312	-0,71154
INHBA	34	279	-245	313	-0,78275
CDKN1B	96	375	-279	471	-0,59236
SOX4	141	443	-302	584	-0,51712
ANKEF1	78	390	-312	468	-0,66667
PTEN	39	433	-394	472	-0,83475

Similarly, a graph depicting the relationship between the membership ratio and the number of targeting miRNAs (rather than the number of experiments as in the previous analysis) was

© 2025 by the author(s). Distributed under a Creative Commons CC BY license.

Preprints.org (www.preprints.org) | NOT PEER-REVIEWED | Posted: 6 June 2025 doi:10.20944/preprints202506.0520.v1

constructed. Only genes targeted by more than 20 miRNAs were included, reducing the dataset from 7,371 to 3,495 genes. A nonlinear threshold, approximating the critical threshold III, was applied to distinguish genes classified as "downregulated" or "upregulated." The resulting gene distribution is presented in Figure 5. Additionally, the figure highlights a subset of genes (10 per category) from database [8], for which experimentally validated interactions relevant to cancer development have been documented.

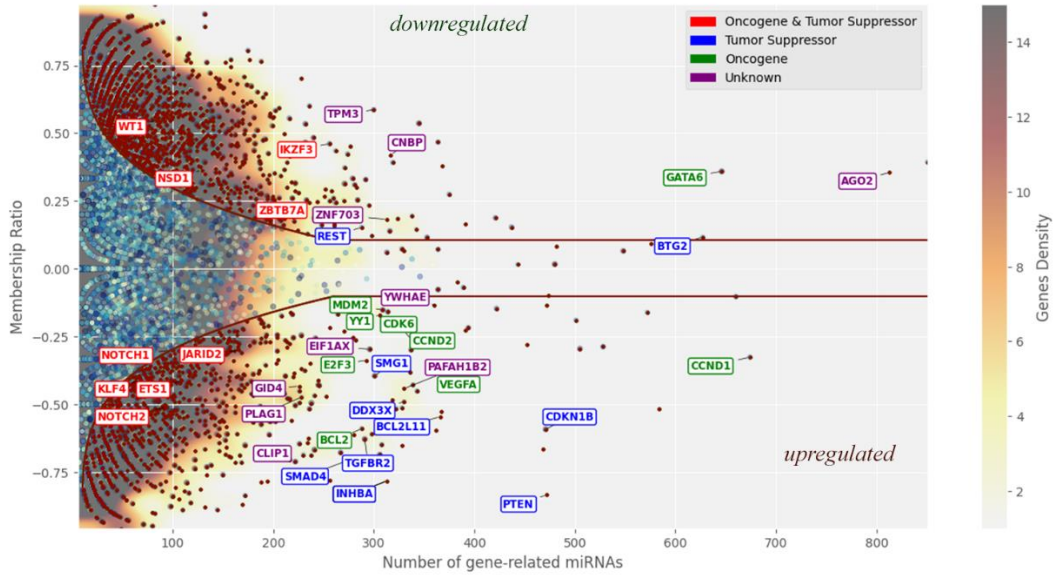

(**a**)

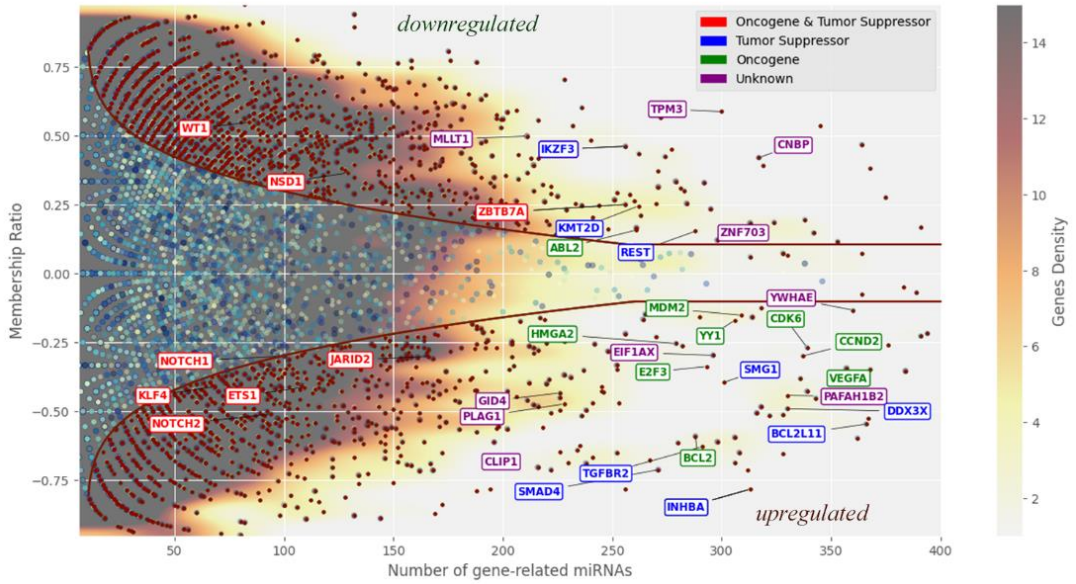

(**b**)

Figure 5. Graph showing the dependence of the membership ratio on the number of miRNAs targeting genes classified as underexpressed or overexpressed (limited to genes targeted by fewer than 20 miRNAs). Panel (a) displays data for genes targeted by up to 800 miRNAs, while panel (b) focuses on genes targeted by up to 400 miRNAs. A subset of genes with experimentally validated roles in cancer development is highlighted.

Table 5, analogous to the miRNA table, presents numerical parameters derived from the graph, including the number of genes above the nonlinear threshold curve for overexpressed and underexpressed categories, the total number of miRNAs targeting these genes, and the cumulative membership ratio for all genes.

© 2025 by the author(s). Distributed under a Creative Commons CC BY license.

Preprints.org (www.preprints.org) | NOT PEER-REVIEWED | Posted: 6 June 2025 doi:10.20944/preprints202506.0520.v1

Table 5. Statistical summary of genes categorized by critical thresholds for underexpressed and overexpressed groups. Notably, the number of downregulated genes is substantially lower than that of upregulated genes.

Parameter	DOWN critical	UP critical
Number of Genes	1922	1281
Number of miRNAs	151 432	118 108
Total sum of Membership Ratios	1106	-731

The data presented in Figure 5 can be utilized for various analyses: investigating individual genes, gene sets, gene categories, or providing a general characterization of gene expression patterns in cancer. Genes positioned above the nonlinear critical threshold, exhibiting a high number of targeting miRNAs (either up- or downregulated) and a membership ratio approaching unity, are of particular interest regarding their involvement in cancer-related mechanisms.

To elucidate the influence of miRNA expression on gene regulation in cancer, gene expression data from database [17], encompassing various cancer types, were analyzed. For each gene, the average expression across all cancer types was calculated, yielding a single representative value (mean log_expression). Concurrently, "critical" genes identified through miRNA expression patterns in Figure 5 were assigned a cumulative membership ratio (div), enabling a two-dimensional representation of gene status. This distribution is illustrated in Figure 6.

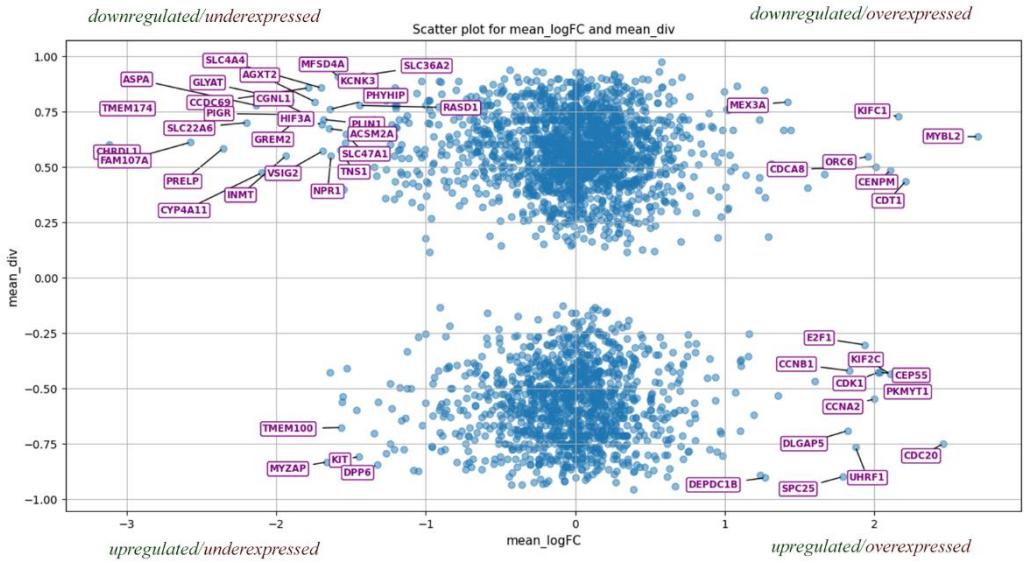

Figure 6. Distribution of genes based on mean logarithmic expression (mean_logFC) across all cancer types and membership ratio (mean_div) derived from miRNA expression data. The 50 genes most distant from the origin are highlighted as an illustrative subset, although the pool of relevant genes extends beyond this. Each quadrant conveys distinct information: Quadrant I: upregulated miRNAs with downregulated genes. Quadrant II: downregulated miRNAs with upregulated genes. Quadrant III: upregulated miRNAs with downregulated genes. Quadrant IV: upregulated miRNAs with downregulated genes. Genes with mean_logFC values near zero exhibit negligible expression. [106].

As illustrated in Figure 6, genes are distributed broadly across the two-dimensional parameter space defined by mean logarithmic expression and membership ratio. Each quadrant corresponds to distinct biological interpretations and potential regulatory mechanisms. Table 6 summarizes the gene counts stratified by cancer type. The first column lists the cancer type, the second column indicates the number of genes with mean log_expression values between –0.1 and 0.1, representing near-zero expression. The third column shows the total number of genes measured for each cancer type, and the fourth column provides the ratio of near-zero expression genes to total measured genes.

© 2025 by the author(s). Distributed under a Creative Commons CC BY license.

Preprints.org (www.preprints.org) | NOT PEER-REVIEWED | Posted: 6 June 2025 doi:10.20944/preprints202506.0520.v1

These genes exhibit negligible expression changes during cancer but are targeted by miRNAs with non-zero membership ratios, suggesting potential miRNA-mediated regulation that is balanced or compensated by other factors. Alternatively, it may indicate that the miRNAs do not directly regulate these genes under the studied conditions.

Table 6. Number of genes exhibiting near-zero average expression for each cancer type, based on miRNA expression data. Notably, certain cancer types such as PRAD, THCA, and PAAD show that nearly one-third of measured genes have negligible expression.

cancer	number_of_zero-expressed genes	sum_of_all_genes	ratio
THYM	465	2890	0,1609
KIRP	678	2952	0,229675
COAD	670	2962	0,226199
CHOL	361	2869	0,125828
BRCA	698	2990	0,233445
BLCA	650	2969	0,218929
UCEC	620	2988	0,207497
GBM	393	2918	0,134681
KICH	547	2893	0,189077
KIRC	665	2988	0,222557
HNSC	664	2949	0,225161
LIHC	727	2929	0,248208
PRAD	975	2954	0,330061
THCA	730	2894	0,252246
LUAD	710	2973	0,238816
READ	527	2861	0,184201
SARC	552	2961	0,186424
PCPG	577	2894	0,199378
PAAD	858	2917	0,294138
LUSC	595	2982	0,199531

The above table provides useful information about genes whose expression remains within the normal range of miRNA concentration. Our main objective is to influence specific genes by modulating the concentration of miRNAs in order to correct the expression levels of a limited set of genes of interest.

At the same time, many genes show clear correlation patterns, as exemplified by the 20 genes located farthest from the origin in the coordinate system.

A subset of 200 individual genes was selected based on having the largest sum of the absolute values of mean log_expression and membership ratio (div). These represent critical genes whose expression may potentially be regulated by changes in the expression of their corresponding miRNAs. Such genes exhibit a clear relationship between their expression in disease and the expression levels of their targeting miRNAs. Of course, it should be noted that gene expression is influenced not only by miRNAs but also by other regulatory factors, so some coincidences may occur.

We then selected miRNAs corresponding to the III non-linear boundary (Figure 2a) that target these 200 critical genes. Among them, there are 634 underexpressed and 462 overexpressed miRNAs, with most miRNAs targeting only one gene from the critical list. For each miRNA from this set, we calculated the number of critical genes it targets. Restricting the analysis to miRNAs targeting at least 10 critical genes, we identified 115 underexpressed and 93 overexpressed miRNAs, which are presented in Table 7 and Figure 7 as examples.

© 2025 by the author(s). Distributed under a Creative Commons CC BY license.

Preprints.org (www.preprints.org) | NOT PEER-REVIEWED | Posted: 6 June 2025 doi:10.20944/preprints202506.0520.v1

Table 7. List of miRNAs influencing genes whose expression patterns correspond to the regulatory effects of these miRNAs. Presented here are the top 10 underexpressed and top 10 overexpressed miRNAs with the highest number of critical gene targets.

miRNA	number_of_genes	miRNA	number_of_genes
hsa-miR-6785-5p	64	hsa-miR-17-5p	61
hsa-miR-149-3p	64	hsa-miR-93-5p	59
hsa-miR-6883-5p	64	hsa-miR-106b-5p	55
hsa-miR-7106-5p	52	hsa-miR-20a-5p	55
hsa-miR-6779-5p	40	hsa-miR-20b-5p	53
hsa-miR-6799-5p	38	hsa-miR-106a-5p	43
hsa-miR-1273h-5p	37	hsa-miR-92a-3p	40
hsa-miR-6825-5p	37	hsa-miR-130b-3p	38
hsa-miR-6780a-5p	37	hsa-miR-21-5p	35

It is assumed that these miRNAs (115 underexpressed and 93 overexpressed) may play a significant role in regulating key mechanisms of cancer development, as they are clearly underexpressed or overexpressed and are likely to influence critical genes whose expression changes have been observed in the presence of cancer and which are targeted by these miRNAs.

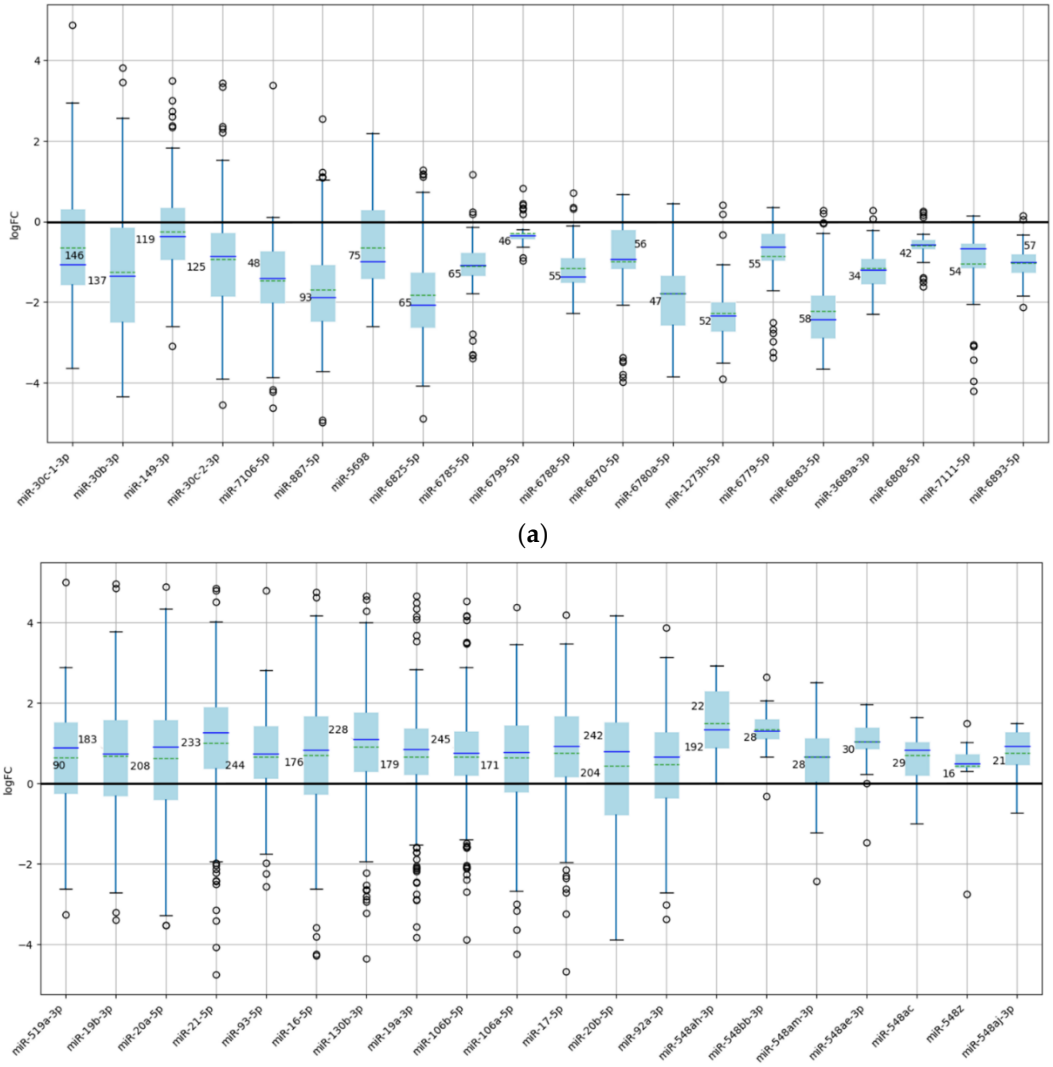

Figure 7. Boxplots for the first 20 underexpressed (a) and 20 overexpressed (b) miRNAs. These specific human miRNAs are of particular interest because they tend to be underexpressed or overexpressed, and their regulatory role is highlighted by the expression levels of the target genes they control.

© 2025 by the author(s). Distributed under a Creative Commons CC BY license.

Preprints.org (www.preprints.org) | NOT PEER-REVIEWED | Posted: 6 June 2025 doi:10.20944/preprints202506.0520.v1

We are primarily interested in genes with a positive membership ratio (div), as these correspond to genes targeted by miRNAs that are significantly underexpressed. These genes have greater practical significance because it is generally more feasible to compensate for insufficient miRNA concentrations (underexpression) than to reduce the levels of overexpressed miRNAs. Among the 115 underexpressed miRNAs identified, only 12 appear in Table 2, whereas 35 of the 93 overexpressed miRNAs are present there. This indicates that changes in the expression of miRNAs and their target genes have been studied more extensively for overexpressed miRNAs compared to underexpressed ones (see Table 8).

Table 8. The names of miRNAs from Table 2 alongside the number of target genes whose expression is significantly altered in the presence of cancer. Panel (a) lists underexpressed miRNAs, while panel (b) lists overexpressed miRNAs. It is evident that only a small subset of underexpressed miRNAs has been studied in detail compared to a larger number of overexpressed miRNAs.

miRNA	number_of_genes
hsa-miR-1-3p	11
hsa-miR-92a-2-5p	10
hsa-miR-125b-5p	8
hsa-miR-30a-5p	6
hsa-miR-483-3p	6
hsa-miR-23a-5p	6
hsa-miR-874-3p	2
hsa-miR-874-5p	2
hsa-miR-206	1
hsa-miR-145-5p	1
hsa-miR-100-5p	1
hsa-let-7b-3p	1

miRNA	number_of_genes
hsa-miR-17-5p	61
hsa-miR-106b-5p	55
hsa-miR-20a-5p	55
hsa-miR-20b-5p	53
hsa-miR-106a-5p	43
hsa-miR-21-5p	35
hsa-miR-16-5p	35
hsa-miR-19b-3p	35
hsa-miR-519a-3p	27
hsa-miR-92b-3p	24
hsa-miR-301a-3p	22
hsa-miR-34a-5p	20
hsa-miR-302c-3p	17
hsa-miR-25-3p	16
hsa-miR-146a-5p	14
hsa-miR-221-3p	13
hsa-miR-222-3p	13
hsa-miR-27a-3p	12
hsa-miR-181b-5p	11
hsa-miR-18a-5p	10
hsa-miR-23a-3p	9
hsa-miR-29b-3p	8
hsa-miR-182-5p	7
hsa-miR-24-3p	7
hsa-miR-106a-3p	6
hsa-miR-17-3p	5
hsa-miR-18b-5p	5
hsa-miR-425-5p	5
hsa-miR-96-5p	5
hsa-miR-146b-5p	5
hsa-miR-2467-3p	3
hsa-miR-19a-5p	2
hsa-miR-372-5p	2
hsa-miR-208b-5p	2
hsa-miR-181b-3p	1

© 2025 by the author(s). Distributed under a Creative Commons CC BY license.

Preprints.org (www.preprints.org) | NOT PEER-REVIEWED | Posted: 6 June 2025 doi:10.20944/preprints202506.0520.v1

3.3. Connection with Plant miRNAs

The next step involved investigating the relationship between plant miRNAs and specific human miRNAs identified in the previous section. Using the critical human miRNAs—607 overexpressed and 786 underexpressed miRNAs defined by the (III) nonlinear separation threshold—we performed a complementarity analysis between plant and critical human miRNAs.

Each plant species has a characteristic set of miRNAs. For each plant, we calculated the average complementarity score, defined as the sum of all complementarity scores with critical human miRNAs divided by the total number of these comparisons [105]. Additionally, average complementarity scores were computed separately for critical overexpressed and critical underexpressed human miRNAs.

Our results show that the average complementarity across all 127 plant species analyzed is approximately ±0.5 for both overexpressed and underexpressed miRNAs. The difference in complementarity between the critical overexpressed and underexpressed groups does not exceed 0.07.

Furthermore, we compared all plant miRNAs against the subset of critical human miRNAs that target critical genes identified previously—specifically, 115 underexpressed and 93 overexpressed miRNAs. The average complementarity-similarity for all plant miRNAs, calculated separately for these two groups of human miRNAs, is summarized in Table 9.

Table 9. Example of the top ten plant miRNAs showing the largest absolute difference in average complementarity when comparing 115 underexpressed and 93 overexpressed critical human miRNAs. This selection highlights some of the most significant plant miRNAs, which could serve as promising candidates for inclusion in plant miRNA panels.

miRNA	coefficient_similarity_up	coefficient_similarity_down	diff
osa-miR2920	0,591405	0,439198	-0,15221
gma-miR5379	0,664349	0,51555	-0,1488
osa-miR2921	0,63002	0,481312	-0,14871
ath-miR407	0,608731	0,4602	-0,14853
osa-miR2122	0,598786	0,460468	-0,13832
pci-miR437	0,617027	0,480315	-0,13671
aly-miR4237	0,59635	0,460316	-0,13603
gma-miR1533	0,509647	0,379024	-0,13062
bdi-miR5057	0,597394	0,467469	-0,12993
osa-miR2875	0,653064	0,524499	-0,12856
miRNA	**coefficient_similarity_up**	**coefficient_similarity_down**	**diff**
ptc-miRf12120-akr	0,567818	0,680251	0,112433
cre-miR914	0,460989	0,573858	0,11287
ptc-miRf10479-akr	0,493849	0,607797	0,113949
ptc-miRf10488-akr	0,529684	0,645046	0,115362
ptc-miRf10495-akr	0,486887	0,603567	0,11668
osa-miR531b	0,459638	0,576326	0,116688
tae-miR2019	0,467059	0,584464	0,117405
peu-miR2911	0,412766	0,542227	0,129461
osa-miR1848	0,442845	0,57365	0,130805
osa-miR531	0,495555	0,635791	0,140237

If the same complementarity analysis is performed for underexpressed and overexpressed miRNAs defined by the III nonlinear threshold, the difference between their average complementarities with plant miRNAs is significantly smaller — see Table 10.

© 2025 by the author(s). Distributed under a Creative Commons CC BY license.

Preprints.org (www.preprints.org) | NOT PEER-REVIEWED | Posted: 6 June 2025 doi:10.20944/preprints202506.0520.v1

Table 10. Examples of the top ten and bottom ten plant miRNAs ranked by the largest absolute differences in mean complementarity when comparing 786 underexpressed and 607 overexpressed human miRNAs at the III nonlinear threshold.

miRNA	coefficient_similarity_up	coefficient_similarity_down	diff
gma-miR1533	0,471812	0,380923	-0,09089
osa-miR2921	0,585374	0,496244	-0,08913
gma-miR1528	0,607889	0,522617	-0,08527
gma-miR5379	0,615216	0,530936	-0,08428
osa-miR2920	0,544466	0,460315	-0,08415
osa-miR2923	0,484547	0,401302	-0,08325
aly-miR4237	0,558946	0,476749	-0,0822
obr-miR812	0,530596	0,451313	-0,07928
gma-miR5031	0,560691	0,481442	-0,07925
osa-miR2875	0,615619	0,537362	-0,07826
miRNA	**coefficient_similarity_up**	**coefficient_similarity_down**	**diff**
ptc-miRf10495-akr	0,540691	0,595738	0,055046
cre-miR1166.1	0,531196	0,587853	0,056656
sbi-miR5384	0,459575	0,516659	0,057084
cre-miR914	0,507068	0,564424	0,057355
ptc-miRf12120-akr	0,610406	0,669192	0,058787
ptc-miRf10625-akr	0,546155	0,605787	0,059631
ptc-miRf10488-akr	0,587835	0,649514	0,061679
osa-miR531b	0,504261	0,567267	0,063006
tae-miR2019	0,518621	0,582685	0,064064
osa-miR1848	0,498489	0,572689	0,0742
osa-miR531	0,553041	0,627539	0,074498

These plant miRNAs may play a crucial role in compensating for the deficiency of underexpressed human miRNAs observed in cancer. Conversely, many plant miRNAs also show average complementarity to overexpressed human miRNAs. From a therapeutic perspective, targeting the restoration of underexpressed human miRNAs appears more promising, as supplementing deficient miRNAs with exogenous counterparts is generally more feasible than attempting to reduce the levels of overexpressed miRNAs. It is also possible to design synthetic miRNAs that maximize complementarity to underexpressed human miRNAs while minimizing binding to overexpressed ones. Furthermore, some plant miRNAs identified here could be key candidates for replacing deficient human miRNAs, although their therapeutic potential requires experimental validation.

4. Discussion

The question arises as to why, despite using a universal approximator like a neural network, we are unable to reliably predict human miRNA expression based solely on its nucleotide sequence. More precisely, predictions can be made, but with an error margin large enough to cast doubt on their practical utility. This likely reflects the fact that miRNA expression depends not only on its sequence but also on a range of other factors—such as interacting molecules or context-specific mechanisms—that significantly influence its regulation. Consequently, the application of neural networks is limited by the heterogeneity of the training data: both the inputs (features) and outputs (expression profiles) vary across individual miRNAs and their specific regulatory contexts, making it difficult to capture universal patterns. Notably, similar levels of prediction error are observed when using purely statistical analyses of miRNA expression data. However, statistical approaches are often more effective at leveraging heterogeneous datasets to uncover robust parameter relationships with a sufficient degree of confidence.

© 2025 by the author(s). Distributed under a Creative Commons CC BY license.

Preprints.org (www.preprints.org) | NOT PEER-REVIEWED | Posted: 6 June 2025 doi:10.20944/preprints202506.0520.v1

5. Conclusions

The conducted analysis demonstrates that the use of exogenous miRNAs, particularly those derived from plants, represents a promising approach to compensate for deficiencies in human miRNA expression associated with cancer. Our findings lay the groundwork for the development of targeted microRNA panels designed for therapeutic and diagnostic applications across a broad spectrum of cancer types. These panels consist of carefully selected sets of plant miRNAs that can potentially be introduced into the body of animals or humans with cancer to restore the balance of miRNA expression.

The methodology for compiling these panels is based on identifying differences between critical and non-critical human miRNAs, considering all types of cancer. Critical miRNAs are defined as those whose expression deviates significantly from normal levels in the presence of cancer, reflecting their important regulatory roles. By targeting these critical miRNAs, the proposed panels aim to modulate gene expression more effectively, addressing the imbalance caused by underexpressed or overexpressed endogenous miRNAs.

Furthermore, our study emphasizes that restoring underexpressed miRNAs is a more feasible and promising therapeutic direction than attempting to suppress overexpressed miRNAs. The complementarity analysis between plant and human miRNAs supports the potential for plant miRNAs to serve as functional substitutes or modulators for human miRNAs with diminished expression in cancer.

Overall, this work provides a comprehensive statistical and bioinformatic foundation for advancing miRNA-based interventions and encourages further experimental validation to confirm the therapeutic efficacy of plant miRNA panels in cancer treatment.

Author Contributions: All the authors contributed to the manuscript. Methodology and validation, M.Z., V.C., P.K., M.M. and D.K.; formal analysis, V.C., M.M., R.B., F.M.Z., S.M. and D.K.; investigation, M.Z., V.C. and M.M.; data curation, M.Z., V.C., M.M., P.K. and D.K.; calculation, M.Z. P.K.; writing-original draft preparation, M.Z. and D.K.; writing-review and editing, M.Z. and D.K.; supervision, M.Z., V.C., M.M. and D.K. All authors have read and agreed to the published version of the manuscript.

Funding: This research received no external funding.

Data Availability Statement: Databases that were used in their original form are available at the links indicated in the work. Generated datasets used and analyzed during the current study are available from the corresponding author upon reasonable request.

Acknowledgments: The authors are grateful for the partial support in writing the chapter in the context of the KATY project of the Horizon 2020 research and innovation program of the European Union, under grant agreement No. 101017453.

Conflicts of Interest: The authors declare no conflicts of interest.

Abbreviations

name	source	name	source
ahy	Arachis hypogaea	han	Helianthus annuus
ptc	Populus trichocarpa	mtr	Medicago truncatula
ppt	Physcomitrella patens	zma	Zea mays
vvi	Vitis vinifera	lja	Lotus japonicus
vun	Vigna unguiculata	smo	Selaginella moellendorffii
tcc	Theobroma cacao	pta	Pinus taeda
stu	Solanum tuberosum	sof	Saccharum officinarum
sly	Solanum lycopersicum	tae	Triticum aestivum
sbi	Sorghum bicolor	ctr	Citrus trifoliata
rco	Ricinus communis	aqc	Aquilegia caerulea

© 2025 by the author(s). Distributed under a Creative Commons CC BY license.

Preprints.org (www.preprints.org) | NOT PEER-REVIEWED | Posted: 6 June 2025 doi:10.20944/preprints202506.0520.v1

osa	Oryza sativa	pvu	Phaseolus vulgaris
gra	Gossypium raimondii	csi	Citrus sinensis
gma	Glycine max	cre	Chlamydomonas reinhardtii
ghr	Gossypium hirsutum	pab	Picea abies
far	Festuca arundinacea	hvu	Hordeum vulgare
bra	Brassica rapa	ssp	Saccharum sp.
bol	Brassica oleracea	rgl	Rehmannia glutinosa
bna	Brassica napus	peu	Populus euphratica
bdi	Brachypodium distachyon	ama	Avicennia marina
ath	Arabidopsis thaliana	gar	Gossypium arboreum
aly	Arabidopsis lyrata	mdo	Monodelphis domestica
		cpa	Carica papaya

References

1. Kaikkonen MU, Lam MT, Glass CK. Non-coding RNAs as regulators of gene expression and epigenetics. Cardiovasc Res. 2011 Jun 1;90(3):430-40. doi: 10.1093/cvr/cvr097. Epub 2011 May 9. PMID: 21558279; PMCID: PMC3096308.
2. Audrius Kilikevicius, Gunter Meister, David R Corey, Reexamining assumptions about miRNA-guided gene silencing, Nucleic Acids Research, Volume 50, Issue 2, 25 January 2022, Pages 617–634, https://doi.org/10.1093/nar/gkab1256
3. Lou, S., Sun, T., Li, H. et al. Mechanisms of microRNA-mediated gene regulation in unicellular model alga Chlamydomonas reinhardtii. Biotechnol Biofuels 11, 244 (2018). https://doi.org/10.1186/s13068-018-1249-y
4. Axtell, M.J., Westholm, J.O. & Lai, E.C. Vive la différence: biogenesis and evolution of microRNAs in plants and animals. Genome Biol 12, 221 (2011). https://doi.org/10.1186/gb-2011-12-4-221
5. Anushree Narjala, Ashwin Nair, Varsha Tirumalai, G Vivek Hari Sundar, Padubidri V Shivaprasad, A conserved sequence signature is essential for robust plant miRNA biogenesis, Nucleic Acids Research, Volume 48, Issue 6, 06 April 2020, Pages 3103–3118, https://doi.org/10.1093/nar/gkaa077
6. Pang LY, Gatenby EL, Kamida A, Whitelaw BA, Hupp TR, Argyle DJ. Global gene expression analysis of canine osteosarcoma stem cells reveals a novel role for COX-2 in tumour initiation. PLoS One. 2014 Jan 8;9(1):e83144. doi: 10.1371/journal.pone.0083144. PMID: 24416158; PMCID: PMC3885401
7. Zheng Y, Liu L, Shukla GC. A comprehensive review of web-based non-coding RNA resources for cancer research. Cancer Lett. 2017 Oct 28;407:1-8. doi: 10.1016/j.canlet.2017.08.015. Epub 2017 Aug 18. PMID: 28823961
8. O'Neill JR, Yébenes Mayordomo M, Mitulović G, Al Shboul S, Bedran G, Faktor J, Hernychova L, Uhrik L, Gomez-Herranz M, Kocikowski M, Save V, Vojtěšek B, Arends M; OCCAMS consortium; Hupp T, Alfaro J. Multi-omic analysis of Esophageal Adenocarcinoma uncovers candidate therapeutic targets and cancer-selective post-transcriptional regulation. Mol Cell Proteomics. 2024 Apr 9:100764. doi: 10.1016/j.mcpro.2024.100764. Epub ahead of print. PMID: 38604503
9. Ali Syeda, Z.; Langden, S.S.S.; Munkhzul, C.; Lee, M.; Song, S.J. Regulatory Mechanism of MicroRNA Expression in Cancer. Int. J. Mol. Sci. 2020, 21, 1723. https://doi.org/10.3390/ijms21051723
10. Otmani K and Lewalle P (2021) Tumor Suppressor miRNA in Cancer Cells and the Tumor Microenvironment: Mechanism of Deregulation and Clinical Implications. Front. Oncol. 11:708765. doi: 10.3389/fonc.2021.708765
11. Zheng Y, Zhu Z. Editorial: Retrieving meaningful patterns from big biomedical data with machine learning approaches. Front Genet. 2023 Mar 17;14:1177996. doi: 10.3389/fgene.2023.1177996. PMID: 37007948; PMCID: PMC10064148
12. Feng Xu#, Yifan Wang#, Yunchao Ling, Chenfen Zhou, Haizhou Wang, Andrew E Teschendorff, Yi Zhao, Haitao Zhao, Yungang He*, Guoqing Zhang*, Zhen Yang*. dbDEMC 3.0: Functional exploration of differentially expressed miRNAs in cancers of human and model organisms. Genomics, Proteomics & Bioinformatics. 2022, 20(3):446-454. doi: 10.1016/j.gpb.2022.04.0062022

© 2025 by the author(s). Distributed under a Creative Commons CC BY license.

Preprints.org (www.preprints.org) | NOT PEER-REVIEWED | Posted: 6 June 2025 doi:10.20944/preprints202506.0520.v1

13. Przybyszewski, J., Malawski, M. & Lichołai, S. GraphTar: applying word2vec and graph neural networks to miRNA target prediction. BMC Bioinformatics 24, 436 (2023). https://doi.org/10.1186/s12859-023-05564-x
14. Hua Hu, Huan Zhao, Tangbo Zhong, Xishang Dong, Lei Wang, Pengyong Han, Zhengwei Li, Adaptive deep propagation graph neural network for predicting miRNA–disease associations, Briefings in Functional Genomics, Volume 22, Issue 5, September 2023, Pages 453–462, https://doi.org/10.1093/bfgp/elad010
15. Seonwoo Min, Byunghan Lee, Sungroh Yoon, TargetNet: functional microRNA target prediction with deep neural networks, Bioinformatics, Volume 38, Issue 3, February 2022, Pages 671–677, https://doi.org/10.1093/bioinformatics/btab733
16. D.Koroliouk, M.Mattei, M.Zoziuk, C.Montesano, R.Bernardini, M.Potestà, L.D.Wondeu, S.Pirrò, A.Galgani, and V.Colizzi. Artificial Intelligence and MicroRNA: Role in Cancer Evolution, Ch.11 in Collective Monograph "Applied AI: Machine Learning, Neural Networks, and Deep Learning. Applications and potentials", Ser.LNEE, Springer. https://link.springer.com/book/9783031612206 (to appear in September 2024).
17. Tang G, Cho M, Wang X (2022) OncoDB: an interactive online database for analysis of gene expression and viral infection in cancer. Nucleic Acids Research, 50(D1):D1334-D1339
18. Cadieux, Z.; Lewis, H.; Esquela-Kerscher, A. Role of Nutrition, the Epigenome, and microRNAs in Cancer Pathogenesis; The Royal Society of Chemistry: London, UK, 2019; Volume 1, pp. 1–35.
19. Dhar, S.; Hicks, C.; Levenson, A.S. Resveratrol and prostate cancer: Promising role for microRNAs. Mol. Nutr. Food Res. 2011, 55, 1219–1229
20. Maleki Dana, P.; Sadoughi, F.; Asemi, Z.; Yousefi, B. The role of polyphenols in overcoming cancer drug resistance: A comprehensive review. Cell Mol. Biol. Lett. 2022, 27, 1.
21. Dhawan A, Scott JG, Harris AL, Buffa FM. Pan-cancer characterisation of microRNA across cancer hallmarks reveals microRNA-mediated downregulation of tumour suppressors. Nat Commun (2018) 9:1–13. doi: 10.1038/s41467-018-07657-1
22. Melnik, B.C. Synergistic Effects of Milk-Derived Exosomes and Galactose on α-Synuclein Pathology in Parkinson's Disease and Type 2 Diabetes Mellitus. Int. J. Mol. Sci. 2021, 22, 1059
23. Melnik, B.C. Lifetime Impact of Cow's Milk on Overactivation of mTORC1: From Fetal to Childhood Overgrowth, Acne, Diabetes, Cancers, and Neurodegeneration. Biomolecules 2021, 11, 404
24. Melnik, B.C.; Schmitz, G. Exosomes of pasteurized milk: Potential pathogens of Western diseases. J. Transl. Med. 2019, 17, 3.
25. Roessler, C.; Kuhlmann, K.; Hellwing, C.; Leimert, A.; Schumann, J. Impact of Polyunsaturated Fatty Acids on miRNA Profiles of Monocytes/Macrophages and Endothelial Cells-A Pilot Study. Int. J. Mol. Sci. 2017, 18, 284.
26. Cannataro, R.; Carbone, L.; Petro, J.L.; Cione, E.; Vargas, S.; Angulo, H.; Forero, D.A.; Odriozola-Martнnez, A.; Kreider, R.B.; Bonilla, D.A. Sarcopenia: Etiology, Nutritional Approaches, and miRNAs. Int. J. Mol. Sci. 2021, 22, 9724
27. El-Sayed, N.S.; Elatrebi, S.; Said, R.; Ibrahim, H.F.; Omar, E.M. Potential mechanisms underlying the association between type II diabetes mellitus and cognitive dysfunction in rats: A link between miRNA-21 and Resveratrol's neuroprotective action. Metab. Brain Dis. 2022, 37, 2375–2388.
28. Wang, X.; Hang, Y.; Liu, J.; Hou, Y.; Wang, N.; Wang, M. Anticancer effect of curcumin inhibits cell growth through miR-21/PTEN/Akt pathway in breast cancer cell. Oncol. Lett. 2017, 13, 4825–4831
29. Li, H.; Jia, Z.; Li, A.; Jenkins, G.; Yang, X.; Hu, J.; Guo, W. Resveratrol repressed viability of U251 cells by miR-21 inhibiting of NF-κB pathway. Mol. Cell Biochem. 2013, 382, 137–143.
30. Rendina, D.; D Elia, L.; Abate, V.; Rebellato, A.; Buondonno, I.; Succoio, M.; Martinelli, F.; Muscariello, R.; De Filippo, G.; D Amelio, P.; et al. Vitamin D Status, Cardiovascular Risk Profile, and miRNA-21 Levels in Hypertensive Patients: Results of the HYPODD Study. Nutrients 2022, 14, 2683
31. Melnik, B.C.; John, S.M.; Carrera-Bastos, P.; Cordain, L.; Leitzmann, C.; Weiskirchen, R.; Schmitz, G. The Role of Cow's Milk Consumption in Breast Cancer Initiation and Progression. Curr. Nutr. Rep. 2023, 12, 122–140

© 2025 by the author(s). Distributed under a Creative Commons CC BY license.

Preprints.org (www.preprints.org) | NOT PEER-REVIEWED | Posted: 6 June 2025 doi:10.20944/preprints202506.0520.v1

32. Baier, S.R.; Nguyen, C.; Xie, F.; Wood, J.R.; Zempleni, J. MicroRNAs are absorbed in biologically meaningful amounts from nutritionally relevant doses of cow milk and affect gene expression in peripheral blood mononuclear cells, HEK-293 kidney cell cultures, and mouse livers. J. Nutr. 2014, 144, 1495–1500
33. Wang, L.; Sadri, M.; Giraud, D.; Zempleni, J. RNase H2-Dependent Polymerase Chain Reaction and Elimination of Confounders in Sample Collection, Storage, and Analysis Strengthen Evidence That microRNAs in Bovine Milk Are Bioavailable in Humans. J. Nutr. 2018, 148, 153–159
34. Zan, L.; Chen, Q.; Zhang, L.; Li, X. Epigallocatechin gallate (EGCG) suppresses growth and tumorigenicity in breast cancer cells by downregulation of miR-25. Bioengineered 2019, 10, 374–382
35. Wang, Y.; Chen, X.; Li, J.; Xia, C. Quercetin Antagonizes Esophagus Cancer by Modulating miR-1-3p/TAGLN2 Pathway-Dependent Growth and Metastasis. Nutr. Cancer 2022, 74, 1872–1881.
36. Farooqi, A.A.; Khalid, S.; Ahmad, A. Regulation of Cell Signaling Pathways and miRNAs by Resveratrol in Different Cancers. Int. J. Mol. Sci. 2018, 19, 652.
37. Kronski, E.; Fiori, M.E.; Barbieri, O.; Astigiano, S.; Mirisola, V.; Killian, P.H.; Bruno, A.; Pagani, A.; Rovera, F.; Pfeffer, U.; et al. miR181b is induced by the chemopreventive polyphenol curcumin and inhibits breast cancer metastasis via down-regulation of the inflammatory cytokines CXCL1 and -2. Mol. Oncol. 2014, 8, 581–595.
38. Norouzi, S.; Majeed, M.; Pirro, M.; Generali, D.; Sahebkar, A. Curcumin as an Adjunct Therapy and microRNA Modulator in Breast Cancer. Curr. Pharm. Des. 2018, 24, 171–177
39. Al-Ansari, M.M.; Aboussekhra, A. miR-146b-5p mediates p16-dependent repression of IL-6 and suppresses paracrine procarcinogenic effects of breast stromal fibroblasts. Oncotarget 2015, 6, 30006–30016
40. Javaid, A.; Zahra, D.; Rashid, F.; Mashraqi, M.; Alzamami, A.; Khurshid, M.; Ali Ashfaq, U. Regulation of micro-RNA, epigenetic factor by natural products for the treatment of cancers: Mechanistic insight and translational association. Saudi J. Biol. Sci. 2022, 29, 103255
41. Song, J.; Jun, M.; Ahn, M.R.; Kim, O.Y. Involvement of miR-Let7A in inflammatory response and cell survival/apoptosis regulated by resveratrol in THP-1 macrophage. Nutr. Res. Pract. 2016, 10, 377–384
42. Tili, E.; Michaille, J.J.; Adair, B.; Alder, H.; Limagne, E.; Taccioli, C.; Ferracin, M.; Delmas, D.; Latruffe, N.; Croce, C.M. Resveratrol decreases the levels of miR-155 by upregulating miR-663, a microRNA targeting JunB and JunD. Carcinogenesis 2010, 31, 1561–1566
43. Ma, F.; Liu, F.; Ding, L.; You, M.; Yue, H.; Zhou, Y.; Hou, Y. Anti-in kV ammatory effects of curcumin are associated with down regulating microRNA-155 in LPS-treated macrophages and mice. Pharm. Biol. 2017, 55, 1263–1273
44. Su, N.; Li, L.; Zhou, E.; Li, H.; Wu, S.; Cao, Z. Resveratrol Downregulates miR-155-5p to Block the Malignant Behavior of Gastric Cancer Cells. BioMed Res. Int. 2022, 2022, 6968641.
45. de la Parra, C.; Castillo-Pichardo, L.; Cruz-Collazo, A.; Cubano, L.; Redis, R.; Calin, G.A.; Dharmawardhane, S. Soy Isoflavone Genistein-Mediated Downregulation of miR-155 Contributes to the Anticancer Effects of Genistein. Nutr. Cancer 2016, 68, 154–164
46. Javed, Z.; Khan, K.; Herrera-Bravo, J.; Naeem, S.; Iqbal, M.J.; Sadia, H.; Qadri, Q.R.; Raza, S.; Irshad, A.; Akbar, A.; et al. Genistein as a regulator of signaling pathways and microRNAs in different types of cancers. Cancer Cell Int. 2021, 21, 388
47. Marques-Rocha, J.L.; Milagro, F.I.; Mansego, M.L.; Zulet, M.A.; Bressan, J.; Martнnez, J.A. Expression of inflammation-related miRNAs in white blood cells from subjects with metabolic syndrome after 8 wk of following a Mediterranean diet-based weight loss program. Nutrition 2016, 32, 48–55
48. Gulei D, Raduly L, Broseghini E, Ferracin M, Berindan-Neagoe I. The extensive role of miR-155 in malignant and non-malignant diseases. Mol Aspects Med (2019) 70:33–56. doi: 10.1016/j.mam.2019.09.004
49. Lei QQ, Huang Y, Li B, Han L, Lv C. MiR-155-5p promotes metastasis and epithelial-mesenchymal transition of renal cell carcinoma by targeting apoptosis-inducing factor. Int J Biol Markers (2020) 36:20–7. doi: 10.1177/1724600820978229
50. Polytarchou C, Iliopoulos D, Hatziapostolou M, Kottakis F, Maroulakou I, Struhl K, et al. Akt2 regulates all akt isoforms and promotes resistance to hypoxia through induction of miR-21 upon oxygen deprivation. Cancer Res (2011) 7113:4720–31. doi: 10.1158/0008-5472.CAN-11-0365

© 2025 by the author(s). Distributed under a Creative Commons CC BY license.

Preprints.org (www.preprints.org) | NOT PEER-REVIEWED | Posted: 6 June 2025 doi:10.20944/preprints202506.0520.v1

51. Jafarifar F, Yao P, Eswarappa SM, Fox PL. Repression of VEGFA by CA-rich element-binding microRNAs is modulated by hnRNP l. EMBO J (2011) 307:1324–34. doi: 10.1038/emboj.2011.38
52. Wang, M.; Liu, K.; Bu, H.; Cong, H.; Dong, G.; Xu, N.; Li, C.; Zhao, Y.; Jiang, F.; Zhang, Y.; et al. Purple sweet potato delphinidin-3-rutin represses glioma proliferation by inducing miR-20b-5p/Atg7-dependent cytostatic autophagy. Mol. Ther. Oncolytics 2022, 26, 314–329
53. Nakano T, Chen I-H, Wang C-C, Chen P-J, Tseng H-P, Huang K-T, et al. Circulating exosomal miR-92b: Its role for cancer immunoediting and clinical value for prediction of posttransplant hepatocellular carcinoma recurrence. Am J Transplant. (2019) 19(12):3250–62. doi: 10.1111/ajt.15490
54. Chiyomaru, T.; Yamamura, S.; Fukuhara, S.; Hidaka, H.; Majid, S.; Saini, S.; Arora, S.; Deng, G.; Shahryari, V.; Chang, I.; et al. Genistein up-regulates tumor suppressor microRNA-574-3p in prostate cancer. PLoS ONE 2013, 8, e58929
55. Ji, X.; Liu, K.; Li, Q.; Shen, Q.; Han, F.; Ye, Q.; Zheng, C. A Mini-Review of Flavone Isomers Apigenin and Genistein in Prostate Cancer Treatment. Front. Pharmacol. 2022, 13, 851589
56. Giangreco, A.A.; Vaishnav, A.; Wagner, D.; Finelli, A.; Fleshner, N.; Van der Kwast, T.; Vieth, R.; Nonn, L. Tumor suppressor microRNAs, miR-100 and -125b, are regulated by 1,25-dihydroxyvitamin D in primary prostate cells and in patient tissue. Cancer Prev. Res. 2013, 6, 483–494
57. Stephan, C.; Ralla, B.; Bonn, F.; Diesner, M.; Lein, M.; Jung, K. Vitamin D Metabolites in Nonmetastatic High-Risk Prostate Cancer Patients with and without Zoledronic Acid Treatment after Prostatectomy. Cancers 2022, 14, 1560.
58. Margolis, L.M.; Carrigan, C.T.; Murphy, N.E.; DiBella, M.N.; Wilson, M.A.; Whitney, C.C.; Howard, E.E.; Pasiakos, S.M.; Rivas, D.A. Carbohydrate intake in recovery from aerobic exercise differentiates skeletal muscle microRNA expression. Am. J. Physiol Endocrinol. Metab. 2022, 323, E435–E447
59. Benameur, T.; Soleti, R.; Porro, C. The Potential Neuroprotective Role of Free and Encapsulated Quercetin Mediated by miRNA against Neurological Diseases. Nutrients 2021, 13, 1318
60. Benameur, T.; Soleti, R.; Porro, C. The Potential Neuroprotective Role of Free and Encapsulated Quercetin Mediated by miRNA against Neurological Diseases. Nutrients 2021, 13, 1318
61. Min, D.; Lv, X.B.; Wang, X.; Zhang, B.; Meng, W.; Yu, F.; Hu, H. Downregulation of miR-302c and miR-520c by 1,25(OH)2D3 treatment enhances the susceptibility of tumour cells to natural killer cell-mediated cytotoxicity. Br. J. Cancer 2013, 109, 723–730.
62. Mucoz, A.; Grant, W.B. Vitamin D and Cancer: An Historical Overview of the Epidemiology and Mechanisms. Nutrients 2022, 14, 1448.
63. Wan Mohd Tajuddin, W.N.B.; Lajis, N.H.; Abas, F.; Othman, I.; Naidu, R. Mechanistic Understanding of Curcumin's Therapeutic Effects in Lung Cancer. Nutrients 2019, 11, 2989
64. Wang, N.; Feng, T.; Liu, X.; Liu, Q. Curcumin inhibits migration and invasion of non-small cell lung cancer cells through up-regulation of miR-206 and suppression of PI3K/AKT/mTOR signaling pathway. Acta Pharm. 2020, 70, 399–409
65. Pan, Y.; Sun, Y.; Liu, Z.; Zhang, C. miR-192-5p upregulation mediates the suppression of curcumin in human NSCLC cell proliferation, migration and invasion by targeting c-Myc and inactivating the Wnt/β-catenin signaling pathway. Mol. Med. Rep. 2020, 22, 1594–1604
66. Monraz-Mendez, C.A.; Escutia-Gutierrez, R.; Rodriguez-Sanabria, J.S.; Galicia-Moreno, M.; Monroy-Ramнrez, H.C.; Sanchez-Orozco, L.; Garcia-Bacuelos, J.; De la Rosa-Bibiano, R.; Santos, A.; Armendariz-Borunda, J.; et al. Moringa oleifera Improves MAFLD by Inducing Epigenetic Modifications. Nutrients 2022, 14, 4225
67. Chai, R.; Xu, C.; Lu, L.; Liu, X.; Ma, Z. Quercetin inhibits proliferation of and induces apoptosis in non-small-cell lung carcinoma via the lncRNA SNHG7/miR-34a-5p pathway. Immunopharmacol. Immunotoxicol. 2021, 43, 693–703
68. Hsieh, P.L.; Liao, Y.W.; Hsieh, C.W.; Chen, P.N.; Yu, C.C. Soy Isoflavone Genistein Impedes Cancer Stemness and Mesenchymal Transition in Head and Neck Cancer through Activating miR-34a/RTCB Axis. Nutrients 2020, 12, 1924

© 2025 by the author(s). Distributed under a Creative Commons CC BY license.

Preprints.org (www.preprints.org) | NOT PEER-REVIEWED | Posted: 6 June 2025 doi:10.20944/preprints202506.0520.v1

69. Cheng L, Xia T-S, Shi L, Xu L, Chen W, Zhu Y, et al. D rhamnose β-hederin inhibits migration and invasion of human breast cancer cell line MDA-MB-231. Biochem Biophys Res Commun (2018) 495(1):775–80. doi: 10.1016/j.bbrc.2017.11.081
70. Tang, Y.; Cao, Y. Curcumin Inhibits the Growth and Metastasis of Melanoma via miR-222-3p/SOX10/Notch Axis. Dis. Markers 2022, 2022, 3129781
71. Yamada, S.; Tsukamoto, S.; Huang, Y.; Makio, A.; Kumazoe, M.; Yamashita, S.; Tachibana, H. Epigallocatechin-3-O-gallate up-regulates microRNA-let-7b expression by activating 67-kDa laminin receptor signaling in melanoma cells. Sci. Rep. 2016, 6, 19225
72. Mlotshwa, S.; Pruss, G.J.; MacArthur, J.L.; Endres, M.W.; Davis, C.; Hofseth, L.J.; Peca, M.M.; Vance, V. A novel chemopreventive strategy based on therapeutic microRNAs produced in plants. Cell Res. 2015, 25, 521–524
73. Xu, J.; Tan, Y.L.; Liu, Q.Y.; Huang, Z.C.; Qiao, Z.H.; Li, T.; Hu, Z.Q.; Lei, L. Quercetin regulates fibrogenic responses of endometrial stromal cell by upregulating miR-145 and inhibiting the TGF-β1/Smad2/Smad3 pathway. Acta Histochem. 2020, 122, 151600.
74. Wei, D.; Yang, L.; Lv, B.; Chen, L. Genistein suppresses retinoblastoma cell viability and growth and induces apoptosis by upregulating miR-145 and inhibiting its target ABCE1. Mol. Vis. 2017, 23, 385–394
75. Liu, H.; Guan, H.; Tan, X.; Jiang, Y.; Li, F.; Sun-Waterhouse, D.; Li, D. Enhanced alleviation of insulin resistance via the IRS-1/Akt/FOXO1 pathway by combining quercetin and EGCG and involving miR-27a-3p and miR-96-5p. Free Radic. Biol. Med. 2022, 181, 105–117
76. Regis S, Caliendo F, Dondero A, Casu B, Romano F, Loiacono F, et al. TGF-ß1 downregulates the expression of CX3CR1 by inducing miR-27a-5p in primary human NK cells. Front Immunol (2017) 8:868. doi: 10.3389/fimmu.2017.00868
77. Donatelli SS, Zhou J-M, Gilvary DL, Eksioglu EA, Chen X, Cress WD, et al. TGF-β-inducible microRNA-183 silences tumor-associated natural killer cells. Proc.Natl. Acad Sci USA (2014) 111(11):4203–8. doi: 10.1073/pnas.1319269111
78. Chen, W.T.; Yang, M.J.; Tsuei, Y.W.; Su, T.C.; Siao, A.C.; Kuo, Y.C.; Huang, L.R.; Chen, Y.; Chen, S.J.; Chen, P.C.; et al. Green Tea Epigallocatechin Gallate Inhibits Preadipocyte Growth via the microRNA-let-7a/HMGA2 Signaling Pathway. Mol. Nutr. Food Res. 2023, 67, e2200336
79. Soheilifar MH, Vaseghi H, Seif F, Ariana M, Ghorbanifar S, Habibi N, et al. Concomitant overexpression of mir-182-5p and mir-182-3p raises the possibility of IL-17–producing treg formation in breast cancer by targeting CD3d, ITK, FOXO1, and NFATs: A metaanalysis and experimental study. Cancer Sci (2021) 112(2):589–603. doi: 10.1111/cas.14764
80. Kang, Q.; Tong, Y.; Gowd, V.; Wang, M.; Chen, F.; Cheng, K.W. Oral administration of EGCG solution equivalent to daily achievable dosages of regular tea drinkers effectively suppresses miR483-3p induced metastasis of hepatocellular carcinoma cells in mice. Food Funct. 2021, 12, 3381–3392
81. Tang Y, Yang J, Wang Y, Tang Z, Liu S, Tang Y. MiR-19b-3p facilitates the proliferation and epithelial-mesenchymal transition, and inhibits the apoptosis of intrahepatic cholangiocarcinoma by suppressing coiled-coil domain containing 6. Arch Biochem Biophys (2020) 6866:108367. doi: 10.1016/j.abb.2020.108367
82. Duchnik, E.; Kruk, J.; Tuchowska, A.; Marchlewicz, M. The Impact of Diet and Physical Activity on Psoriasis: A Narrative Review of the Current Evidence. Nutrients 2023, 15, 840
83. Saini, S.K.; Singh, A.; Saini, M.; Gonzalez-Freire, M.; Leeuwenburgh, C.; Anton, S.D. Time-Restricted Eating Regimen Differentially Affects Circulatory miRNA Expression in Older Overweight Adults. Nutrients 2022, 14, 1843
84. Melnik, B.C. Lifetime Impact of Cow's Milk on Overactivation of mTORC1: From Fetal to Childhood Overgrowth, Acne, Diabetes, Cancers, and Neurodegeneration. Biomolecules 2021, 11, 404
85. Ghosh S, Bhowmik S, Majumdar S, Goswami A, Chakraborty J, Gupta S, et al. The exosome encapsulated microRNAs as circulating diagnostic marker for hepatocellular carcinoma with low alpha-fetoprotein. Int J Cancer (2020) 147(10):2934–47. doi: 10.1002/ijc.33111
86. Luan G, Wang M, Yuan J, Bu X, Song J, Wang C, et al. Regulatory network identified by pulmonary transcriptome and proteome profiling reveals extensive change of tumor − related genes in microRNA − 21 knockout mice. J Cancer Res Clin Oncol (2022) 148(8):1919–29. doi: 10.1007/s00432-022-03967-6

© 2025 by the author(s). Distributed under a Creative Commons CC BY license.

Preprints.org (www.preprints.org) | NOT PEER-REVIEWED | Posted: 6 June 2025 doi:10.20944/preprints202506.0520.v1

87. Hu Y, Wang C, Li Y, Zhao J, Chen C, Zhou Y, et al. MiR-21 controls in situ expansion of CCR6 + regulatory T cells through PTEN/AKT pathway in breast cancer. Immunol Cell Biol (2015) 93(8):753–64. doi: 10.1038/icb.2015.37
88. Levens D. Disentangling the MYC web. Proc Natl Acad Sci USA (2002) 999:5757–9. doi: 10.1073/pnas.102173199
89. Liang YK, Lin H-Y, Dou X-W, Chen M, Wei X-L, Zhang Y-Q, et al. MiR-221/222 promote epithelial-mesenchymal transition by targeting Notch3 in breast cancer cell lines. NPJ Breast Cancer (2018) 4:20. doi: 10.1038/s41523-018-0073-7
90. Zhang Y, Zhang D, Lv J, Wang S, Zhang Q. miR-410–3p promotes prostate cancer progression via regulating PTEN/AKT/mTOR signaling pathway. Biochem Biophys Res Commun (2018) 503:2459–65. doi: 10.1016/j.bbrc.2018.06.176
91. Souza MF, Cólus IMS, Fonseca AS, Antunes VC, Kumar D, Cavalli LR. MiR-182-5p modulates prostate cancer aggressive phenotypes by targeting EMT associated pathways. Biomolecules (2022) 12:187. doi: 10.3390/biom12020187
92. Ma ZH, Shi PD, Wan BS. MiR-410-3p activates the NF-κB pathway by targeting ZCCHC10 to promote migration, invasion and EMT of colorectal cancer. Cytokine (2021) 1401:155433. doi: 10.1016/j.cyto.2021.155433
93. Gao F, Zhao Z-L, Zhao W-T, Fan Q-R, Wang S-C, Li J, et al. MiR-9 modulates the expression of interferon-regulated genes and MHC class I molecules in human nasopharyngeal carcinoma cells. Biochem Biophys Res Commun (2013) 431:610–6. doi: 10.1016/j.bbrc.2012.12.097
94. Cheng WC, Liao T-T, Lin C-C, Yuan L-TE, Lan H-Y, Lin H-H, et al. RAB27B-activated secretion of stem-like tumor exosomes delivers the biomarker microRNA-146a-5p, which promotes tumorigenesis and associates with an immunosuppressive tumor microenvironment in colorectal cancer. Int J Cancer (2019) 145:2209–24. doi: 10.1002/ijc.32338
95. Xu D, Han Q, Hou Z, Zhang C, Zhang J. MIR-146a negatively regulates NK cell functions via STAT1 signaling. Cell Mol Immunol (2017) 14(8):712–20. doi: 10.1038/cmi.2015.113
96. Yang W, Yang S, Zhang F, Cheng F, Wang X, Rao J. Influence of the hippo-YAP signaling pathway on tumor associated macrophages (TAMs) and its implications on cancer immunosuppressive microenvironment. Ann Transl Med (2020) 8:399–9. doi: 10.21037/atm.2020.02.11
97. Liu J, Fan L, Yu H, Zhang J, He Y, Feng D, et al. Endoplasmic reticulum stress causes liver cancer cells to release exosomal miR-23a-3p and up-regulate programmed death ligand 1 expression in macrophages. Hepatology (2019) 70:241–58. doi: 10.1002/hep.30607
98. Stern-Ginossar N, Gur C, Biton M, Horwitz E, Elboim M, Stanietsky N, et al. Human microRNAs regulate stress-induced immune responses mediated by the receptor NKG2D. Nat Immunol (2008) 9(9):1065–73. doi: 10.1038/ni.1642
99. Breunig C, Pahl J, Küblbeck M, Miller M, Antonelli D, Erdem N, et al. MicroRNA-519a-3p mediates apoptosis resistance in breast cancer cells and their escape from recognition by natural killer cells. Cell Death Dis (2017) 8:e2973. doi: 10.1038/cddis.2017.364
100. Chen WX, Cheng L, Pan M, Qian Q, Zhu Y-L, Xu L-Y, et al. D rhamnose β-hederin against human breast cancer by reducing tumor-derived exosomes. Oncol Lett (2018) 16(4):5172–8. doi: 10.3892/ol.2018.9254
101. Ning T, Li J, He Y, Zhang H, Wang X, Deng T, et al. Exosomal miR-208b related with oxaliplatin resistance promotes treg expansion in colorectal cancer. Mol Ther (2021) 29(9):2723–36. doi: 10.1016/j.ymthe.2021.04.028
102. Kahroba H, Samadi N, Mostafazadeh M, Hejazi MS, Sadeghi MR, Hashemzadeh S, et al. Evaluating the presence of deregulated tumoral onco-microRNAs in serum-derived exosomes of gastric cancer patients as noninvasive diagnostic biomarkers. BioImpacts (2021) 12(2):127–38. doi: 10.34172/bi.2021.22178
103. Yuhao Chen and Xiaowei Wang (2020) miRDB: an online database for prediction of functional microRNA targets. Nucleic Acids Research. 48(D1):D127-D131

© 2025 by the author(s). Distributed under a Creative Commons CC BY license.

Preprints.org (www.preprints.org) | NOT PEER-REVIEWED | Posted: 6 June 2025 doi:10.20944/preprints202506.0520.v1

104. Hsi-Yuan Huang, Yang-Chi-Dung Lin, Shidong Cui, Yixian Huang, Yun Tang, Jiatong Xu, Jiayang Bao, Yulin Li, Jia Wen, Huali Zuo, Weijuan Wang, Jing Li, Jie Ni, Yini Ruan, Liping Li, Yidan Chen, Yueyang Xie, Zihao Zhu, Xiaoxuan Cai, Xinyi Chen, Lantian Yao, Yigang Chen, Yijun Luo, Shupeng LuXu, Mengqi Luo, Chih-Min Chiu, Kun Ma, Lizhe Zhu, Gui-Juan Cheng, Chen Bai, Ying-Chih Chiang, Liping Wang, Fengxiang Wei, Tzong-Yi Lee, Hsien-Da Huang, miRTarBase update 2022: an informative resource for experimentally validated miRNA–target interactions, Nucleic Acids Research, Volume 50, Issue D1, 7 January 2022, Pages D222–D230, https://doi.org/10.1093/nar/gkab1079
105. Zhenhai Zhang, Jingyin Yu, Daofeng Li, Zuyong Zhang, Fengxia Liu, Xin Zhou, Tao Wang, Yi Ling, and Zhen Su, PMRD: plant microRNA database, Nucleic Acids Research, 2010, Vol. 38, Database issue D806-D813
106. Zoziuk, M.; Colizzi, V.; Krysenko, P.; Mattei, M.; Bernardini, R.; Zanzotto, F.M.; Marini, S.; Koroliouk, D. Plant miRNAs for Improved Gene Regulation in a Wide Range of Human Cancers. *Curr. Issues Mol. Biol.* **2025**, *47*, 42. https://doi.org/10.3390/cimb47010042

Disclaimer/Publisher's Note: The statements, opinions and data contained in all publications are solely those of the individual author(s) and contributor(s) and not of MDPI and/or the editor(s). MDPI and/or the editor(s) disclaim responsibility for any injury to people or property resulting from any ideas, methods, instructions or products referred to in the content.

© 2025 by the author(s). Distributed under a Creative Commons CC BY license.